Assessing the hydrological response from an ensemble of CMIP5 climate projections in the transition zone of the Atlantic region (Bay of Biscay).

Maite Meaurio(a), Ane Zabaleta(a), Laurie Boithias(b,c), Ane Miren Epelde(a), Sabine Sauvage(b), Jose-Miguel Sanchez-Perez(b), Raghavan Srinivasan(d), Iñaki Antigüedad(a).

(a) Hydrogeology and Environment Group, Science and Technology Faculty, University of the Basque Country UPV/EHU, 48940 Leioa, Basque Country, Spain

(b) EcoLab, Université de Toulouse, CNRS, INPT, UPS, 31400 Toulouse, France

(c) Géosciences Environnement Toulouse, Université de Toulouse, CNES, CNRS, IRD, UPS, 31400 Toulouse, France

(d) Spatial Sciences Laboratory, Texas A&M University (TAMU), 77843 College Station, Texas, USA.

*Corresponding author information:

Maite Meaurio

e-mail address: maite.meaurio@ehu.eus

Abstract

The climate changes projected for the 21st century will have consequences on the hydrological response of catchments. These changes, and their consequences, are most uncertain in the transition zones. The study area, in the Bay of Biscay, is located in the transition zone of the European Atlantic region where hydrological impact of climate change has been scarcely studied. To assess the hydrological effects of climate change, 16 climate scenarios including 5 General Circulation Models (GCM) from the 5º report of the Coupled Model Intercomparison Project (CMIP5), 2 statistical downscaling methods and 2 Representative Concentration Pathways were considered in a hydrological model (SWAT). Projections for future discharge (2011-2100) were divided into three 30-year horizons (2030s, 2060s and 2090s) and a comparison was made between these horizons and the baseline (1961-2000). The results show that the downscaling method used resulted in a higher source of uncertainty than GCM itself. In addition, the uncertainties inherent to the methods used at all the levels do not affect the results equally along the year. In spite of those uncertainties, general trends for the 2090s predict seasonal discharge decreases by around -17% in autumn, -16% in spring, -11% in winter and -7% in summer. These results are in line with those predicted for France and the Iberian Peninsula in the Atlantic region. Trends for extreme flows were also analysed: the most significant trend shows an increase in the duration (days) of low flows. From an environmental point of view, and considering the need to meet the objectives established by the European Water Framework Directive (WFD), this would be a drawback for the future planning on water management.

Keywords: CMIP5, hydrological trend, high flow and low flow, SWAT model, Atlantic region, transition zone.

Highlights:

Hydrological impact studies scarcity in transition zone of Atlantic region addressed

Downscaling method used resulted in a higher source of uncertainty than GCM itself

Results in line with those predicted for Atlantic region (France, Iberian Peninsula)

Uncertainties inherent to methods used do not affect results equally along the year

Highest decrease in low flows is a drawback for future planning on water management

1. Introduction

Climate change will have effects on hydrological systems, which in turn will impact ecological, social and economic systems (Bender et al., 1984; Dibike and Coulibaly, 2005; Brauman et al., 2007; Vörösmarty et al., 2010). These effects can be studied both at local and regional levels, providing important information for territorial and sectoral planning (Lahmer et al., 2001). In some areas where water scarcity is not a key aspect of the territorial management, as it is the case of the Basque Country (Bay of Biscay, Cantabrian Sea), few studies have been carried out to evaluate the possible effects of the climate change on catchment hydrology.

The most commonly used method for evaluating climate change impact on hydrological systems is to introduce General Circulation Models (GCMs) into hydrological models (Gosling et al., 2011). This provides a good tool for studying the relationship between climate and water resources, considering also the effect of human activities (Jothityangkoon et al., 2001; Leavesley, 1994). However, GCMs usually have little spatial resolution and if they are introduced directly into hydrological models, the performance is poor (Fowler et al., 2007). This is the reason for the need of performing a statistical or dynamical downscaling of general circulation models.

Uncertainties related to the impact of climate change appear at the four levels of the sequence: GCMs, Representative Concentration Pathway (RCP) or emission scenario, downscaling and hydrologic projections. For example, Chen et al. (2011) assessed the uncertainty of downscaling methods and the results showed that impact studies based on only one downscaling method should be interpreted with caution. Wilby (2005) found that the uncertainty related to hydrological model calibration is comparable with that involved in greenhouse and other pollutant emissions. Wilby and Harris (2006) determined that the greatest uncertainties derive more from the choice of GCM and downscaling methods and less from the hydrological models and emission scenarios. Some research supports the argument that the choice of hydrological model has a relatively minor impact on the results of hydrological simulations based on climate projections (Boyer et al., 2010; Bates et al., 2008; Kay et al., 2006) and major uncertainties come from the GCM structure (Arnell, 1999; Bergstrom et al., 2011; Nijssen et al., 2001; Kay et al., 2009; Chen et al., 2011; Arnell et al., 2011; Teng et al., 2012). For this reason, the use of an ensemble of climate models gives a better estimate of uncertainty (e.g. IPCC, 2007, 2013; Johnson and Sharma, 2009; Stahl et al., 2011). Therefore, the inherent uncertainties of the methods used at each of these levels propagate the uncertainties of the previous levels of the sequence, with the result that all single uncertainties are then propagated in the hydrological models (Wilby et al., 2006).

Europe is a representative region of global changes due to climate warming (Shorthouse and Arnell, 1999). There is a clear contrast between the north and the south of the continent, hence, an increase in precipitation and, therefore, an increase in water discharge, has been pointed out in the north (e.g. Arnell, 1998; Kiely, 1999; Xu and Halldin, 1997; IPCC, 2007, 2014). By contrast, in the south the trend is reversed: a decrease of precipitation is predicted and, consequently, a decrease in discharge (e.g. Mimikou et al., 2000; Ayala-Carcedo and Iglesias, 2000; Ribalaygua et al., 2013; Lespinas et al., 2014; Touhami et al., 2015; Valverde et al., 2015; IPCC, 2014). Due to its location in the Bay of Biscay (Fig. 1), the arid climatological conditions projected for southern Europe do not seem to be representative for the Basque Country. However, neither is it clear that the hydrological changes projected in this area will follow the discharge increasing trend projected for northern Europe. In this sense, Coch and Mediero (2015) analyzed low flows to identify different areas of hydrologic trends of the Iberian Peninsula and Mediero et al. (2015) investigated the flood-prone regions in Europe. Both studies reached the same conclusion: The Basque Country area would be located in the Atlantic region. This area is characterized by Atlantic frontal systems coming from the west, usually from autumn to spring, being summer the dry season. Furthermore, the 4th report of the International Panel on Climate Change (IPCC, 2007) provides a vulnerability map of Europe for the XXI century, where the Atlantic region encompasses the northern Iberian Peninsula, western France, the Netherlands, Belgium, northern part of Germany, western Denmark and the UK. As a general trend, the report predicts an increase in the future winter storms and flooding for this region.

Research works conducted since 2000 in the Atlantic region to evaluate the impacts of climate change in the water resources are summarized in Table 1. This table was done to identify possible future hydrological trends in this region, thus, research works that were published in high impact journals and some reports were collected. In addition, to have a homogeneous view, the selection was made only with works that presented their results in mean discharge difference (%) with respect to their baseline. When necessary, mean difference values and ranges were calculated (for example to obtain seasonal values from monthly ones). Despite some seasonal trends in Table 1 are difficult to interpret, general trends of mean discharge evolution can be derived considering those more clearly observed. A significant decrease of discharge is observed in all the studies for summer and spring seasons. This decrease is even more important towards the end of the century. In winter trends are not so clear. In the UK (b, in Table 1) and in the Iberian Peninsula (d, Table 1), both increase and decrease discharge can be expected depending on the study, whereas in France (c,

Table 1) the observed trend is decreasing. Trends in spring are similar to those in winter though decrease of discharge prevails. Annual trends are determined by trends in winter and spring.

From the aforementioned research works (Table 1), it can be deduced the general idea that a transition zone exists between northern and southern Atlantic region, where expected trends in discharge (in winter and spring) change from increasing in the north to decreasing in the south. It is not an easy task to locate this zone, due to the low spatial resolution of climate models; according to Habets et al. (2013) this zone is located in northern France and following IPCC (2007) and Goubanova and Li (2007) it would be in the north of the Iberian Peninsula, that includes the study region. The uncertainties involved, precisely, in the climate predictions for that transition zone are large and difficult to identify. Therefore, it should be an in-depth studied area. However, compared with other European regions, the number of research works in this zone is low (Table 1); this evidences the strength of the current work.

In this context, the aim of this study is to assess the possible future effects of climate change on the hydrology of a catchment located in the Atlantic region of the Iberian Peninsula. For this purpose, five GCMs of the 5º report of the Coupled Model Intercomparison Project (CMIP5), two downscaling methods and two RCPs were considered, using a total of 16 climate projections (Table 2).

The projected climate variables were introduced in the Soil and Water Assessment Tool or SWAT model (Arnold et al., 1998) to evaluate the hydrological impact of climate change, focusing on the following partial objectives:

1) To evaluate the baselines of considered downscaled projections of climate variables with respect to the observed data (1961-2000).

2) To study the average hydrological impact of future climate projections in three horizons: 2030s for 2011-2040, 2060s for 2041-2070, 2090s for 2071-2100 (annual, seasonal and monthly).
3) To assess possible trends in extreme daily discharges (2011-2100) and compare the observed figures for the reference period (1961-2000).
4) To identify the differences between climate projections and identify the greatest uncertainties in the different steps of the followed methodology.

2. Methodology

2.1. Description of the study area

The study area is the catchment of the Upper Nerbioi River (185 km^2), which is located in the centre-west of the Basque Country (Bay of Biscay), at an average latitude of 43º and longitude of 3º (Fig. 1). Its direction South-North, is very common in catchments of the Basque Country, as well as its geology and land use. The catchment is located at the interface between the Atlantic climate in the north and the Mediterranean climate in the south. In addition, this is one of the catchments with longest records of discharge series in this zone.

Average annual rainfall is about 1,000 mm and it is distributed quite evenly throughout the year: close to 300 mm in winter and autumn; 230 mm in spring and 30 mm in summer, as an average (1961-2014). The mean annual temperature is around 12 °C, being the seasonal averages for winter and summer 8 ºC and 20 ºC (1961-2014), respectively.

The mean elevation of the catchment is around 200 m above sea level (m.a.s.l.) (Fig. 1). The lithology is dominated by siltstones, clays and sandstones with medium-low permeability (Geographical Database of the Basque Government, www.geoeuskadi.net). In the southeast part, at an average altitude of 1,100 m.a.s.l., there is a highly permeable late Cretaceous limestone platform. The main soil types are Cambisols, Rankers and Gleysols (FAO, 1977), which are characterized by high clay and silt contents. Land use in the catchment is divided into native forests, exotic plantations and pasturelands. The areas with the highest slopes (>35%) are covered by forest and tree plantations, while the flatter areas (7-15%) host pasturelands. The average slope in the catchment is around 17%. It should be noted that possible future changes in land use have not been taken into consideration in this work.

Mean annual discharge at the outlet of the catchment is 3 $m^3 s^{-1}$. The mean in spring and autumn is around 3.5 $m^3 s^{-1}$; in winter 5 $m^3 s^{-1}$ and in summer 0.8 $m^3 s^{-1}$ (1996-2013). Discharge data from a gauging station (Gardea; http://www.bizkaia.eus) located at the outlet of the catchment (Fig. 1) were used in this work to calibrate and validate the hydrological model. Discharge data have been recorded at this gauging station since 1995. This station was designed to precisely measure mean and high flows.

2.2. Description of the hydrological model: SWAT

The SWAT model is a basin-scale continuous in time and semi-distributed model operating on a daily time step. It was developed to evaluate the impact of management practices on water, sediment and agricultural chemical yields in ungauged basins (Arnold et al., 1998). It can be used in a broad range of conditions and it has already been widely used to study the impacts of environmental and climate change (e.g. Bouraoui et al., 2002; Li et al., 2009; Abbaspour et al., 2009; Bekele and Knapp, 2010; Zhang et al., 2014).

SWAT divides the catchment into sub-basins which are subdivided into Hydrological Response Units (HRUs) with homogeneous land use, soil characteristics and slope gradient. Two methods are used to simulate surface runoff in the SWAT model: the modified SCS curve number (USDA Soil Conservation Service, 1972) and the Green-Ampt infiltration method (Green and Ampt, 1911), which requires a sub-daily precipitation time step. In this case the observed meteorological data used to calibrate and validate the model were daily and therefore the SCS method was used. The model calculates the peak runoff rate with a modified rational method (Chow et al., 1988). The lateral subsurface flow in the soil profile is determined for each soil layer, using the kinematic storage routing model (Sloan and Moore, 1984), which is calculated simultaneously with percolation. The groundwater flow contribution to the total streamflow is simulated by creating shallow aquifer storage (Arnold and Allen, 1996) where percolation from the bottom of the root zone is considered as recharge to the shallow aquifer. The potential evapotranspiration can be estimated using the Hargreaves (Hargreaves and Samani, 1985), Priestley-Taylor (Priestley and Taylor, 1972) and Penman-Monteith (Monteith, 1965) methods. This study uses Hargreaves, which only requires precipitation and maximum and minimum temperature, since these were the only meteorological data available. The flow is routed through the channel using either the variable storage coefficient method (Williams, 1969) or the Muskingum routing method (Overton, 1966). In this study the former method was used because it better suited the observed discharge.

2.3. Hydrological model input and data source.

SWAT requires topographic, land use/cover, soil and meteorological data. The source for the Digital Elevation Model (LIDAR 2008, 5x5m), land use classification (2005, 1: 10,000) and part of the soil map (1: 25,000) is the Basque Government's Geographical Database (www.geoeuskadi.net). The remainder of the soil map was obtained from the soil map of Araba province (1:200,000) (Iñiguez et al., 1980). Soil properties were obtained from these two sources and the plant growth properties for each land cover were directly obtained from the SWAT database.

For the calibration and the validation of the model, daily maximum and minimum temperature and precipitation (1996-2013) for the Gardea (G067), Saratxo (G040) and Amurrio (AEMET 1060) meteorological stations were used (Fig. 1). The meteorological data for the Gardea and Saratxo stations and the daily observed discharge for the Gardea G067 gauging station (Fig. 1) were obtained from the Basque Meteorological Agency (www.euskalmet.euskadi.eus) and Bizkaia Provincial Council (http://www.bizkaia.eus), while the meteorological data for Amurrio were provided by the Spanish Meteorological Agency (AEMET). The climate variables of the daily maximum and minimum temperature and precipitation used to model the climate scenarios were downloaded from the AEMET website (http://escenarios.aemet.es/). These climate variables were given for Amurrio meteorological station (AEMET 1060) (Fig. 1) for baseline periods (1961-2000 for each GCM) and future scenarios (2006-2100). For the baseline period there is a small number of years with available discharge data (1995-2000). However, for Amurrio station (AEMET 1060), previous observed meteorological data (1961-2000) are available. We used them to generate (using SWAT) discharge series from 1961-2000. The modeled series was termed OBS_SIM.

2.4. SWAT calibration, validation and evaluation

Daily river flow ($m^3 s^{-1}$) observed at the Gardea G067 gauging station was used for the model calibration and validation. The model was run daily; the period from 1996 to 2006 was used for calibration and the period from 2007 to 2013 for validation. The purpose of this selection of the calibration and validation years was to consider similar hydro-meteorological conditions for both periods (Fig. 2). The 18 years of simulation ensures that wet, dry and average years are all included.

The first step in calibration was to identify the most sensitive parameters for the catchment. To achieve this, a “one-at-a-time” sensitivity analysis (van Griensven et al.,

2006) was conducted with 22 flow-related parameters. The most sensitive parameters are listed in Table 3. Later, a realistic value-range was introduced for the most sensitive parameters in the SWAT CUP program (Abbaspour et al., 2007a) to make an autocalibration using the SUFI2 algorithm (Abbaspour et al., 2004, 2007a) (Table 3). The program calculates a p-factor to quantify the degree of uncertainty of each iteration. The p-factor is the percentage of measured data bracketed by the 95% prediction uncertainty (95PPU). A value of 1 indicates 100% bracketing of the measured data. The r-factor is the average thickness of the 95PPU band divided by the standard deviation of the measured data. The r-factor seeks to bracket most of the measured data with the smallest possible value (Abbaspour et al., 2007b). A working value of >0.7 for p-factor and <1.5 for r-factor is recommended (Abbaspour et al., 2015). In this way, besides achieving good results for the calibration, the uncertainty of the simulation is also quantified. Finally, the validation process was performed using the parameter set for the calibration period and comparing the observed and simulated discharge (2007-2013).

To evaluate the performance of the model (for calibration and validation), several evaluation criteria were used: Nash-Sutcliffe efficiency (NSE) (Nash and Sutcliffe, 1970), the coefficient of determination (r^2) and its slope, the percent bias (PBIAS) (Gupta et al., 1999) and the ratio of the root mean square error to the standard deviation of measured data (RSR) (Moriasi et al., 2007). According to these authors, the discharge simulation is satisfactory in a monthly time step when NSE>0.5, r^2>0.5 and the slope and intercept of the linear regression between simulated and observed discharges are close to 1 and 0 respectively (Arnold et al., 2012), RSR≤0.7, and PBIAS<25%. In addition to this and in order to ensure the goodness of the modeling process and determine its uncertainty for future hydrological projections, these statistical indices were also used in differentiated climate conditions. Considering that future climate scenarios often project a more extreme climate than that observed in recent decades for the North of the Iberian Peninsula (e.g. Brunet et al, 2009; CEDEX, 2010; IPCC, 2013), as proposed by Brigode et al. (2012), the 3 consecutive driest and wettest years were chosen to analyze whether the calibrated model is able to correctly simulate extreme conditions. The driest and wettest years were selected by calculating an "Aridity Index" (hereafter AI) for all the available data (1996-2013), where this index is deemed to be the ratio between potential evapotranspiration and precipitation (Görgen et al., 2010; Brigode et al., 2012). The three consecutive calendar years with the lowest AI are 2003, 2004 and 2005 while the years with the highest AI value are 2010, 2011 and 2012. Thus, using the model evaluation methods for daily discharge in different time periods (annually and seasonally) and in years with low and high AI, it is possible to evaluate whether the performance of the model is good enough to simulate the future climate projections and also to identify where the largest uncertainties are.

2.5. Selection and evaluation of climate scenarios

To deal with the problem of spatial resolution of climate models, AEMET has downscaled some GCMs for the Coupled Model Intercomparison Project Phase 5 (CMIP5). The statistical downscaling methods links the results of GCMs or RCMs (predictors) with simultaneous historical data (predictands) observed on a much smaller scale (Brands et al., 2011; Hewitson and Crame, 1996; Wilby and Wigley, 1997; Zorita and von Storch, 1999; Maraun et al., 2010). The main drawback of these downscaling methods is the assumption that future climate variability will be the same as in the past (Brunet et al., 2009). The statistical downscaling methods applied in the GCMs are the AEMET analogues (AN) (Petisco and Martín, 2006) and the Statistical Downscaling Method (SDSM) (Wilby et al., 2002).

From all the GCMs downscaled by AEMET (Table 2), a selection of 5 was made for this paper. For that purpose, firstly, the results of research works such as that by Perez et al. (2014) were taken into consideration -there, the CMIP5 models performance is evaluated for the north-east Atlantic region-. Secondly, the meteorological data for the climate projection baselines (1961-2000) of 9 GCMs (downscaled with AN and SDSM methods) were compared to the data observed at the Amurrio (AEMET 1060) station (Fig.1), selecting those that best fitted.

In order to provide some patterns of changes in the composition of the atmosphere, a set of known scenarios or paths called "Representative Concentration Pathways" (RCPs) were defined by the research community (Meinshausen et al., 2011; van Vuuren et al., 2011; IPCC, 2013). These are based on the future radiative forcing of the atmosphere. Two of the most widely used RCPs downscaled by AEMET are the mitigation scenario (RCP 4.5) and the high emission scenario (RCP 8.5). In the RCP 4.5 scenario, radiative forcing is stabilized before 2100 at 4.5 W m^{-2} through the use of a range of technologies and strategies to reduce greenhouse gas emissions. The RCP 8.5 scenario, on the other hand, is characterized by increasing greenhouse gas emissions with radiative forcing in 2100 of 8.5 W m^{-2} (Moss et al., 2010; Taylor et al., 2012).

AEMET supplies daily climate variables for the Amurrio (AEMET 1060) meteorological station (Fig. 1), for each downscaled GCM for the baseline period (1961-2000) and for future climate projections (2006-2100). In order to consider the uncertainty inherent to climate projections in the resulting hydrologic projections, this paper draws on 5 GCMs (ACCESS1-0, BNU-ESM, MPI-ESM-RL, MPI-ESM-MR, CMCC-CESM), 2 RCPs (8.5 and 4.5) and 2 downscaling methods (AN and SDSM). As it has been widely recognized, an ensemble of different scenarios gives more reliable results than single-model simulations (Boorman and Sefton, 1997; Giorgi and Mearns, 2002; Murphy et al., 2004; IPCC, 2007, 2013). With these combinations, 16 climate projections were implemented, as shown in Table 2.

As mentioned above, in order to select the downscaled GCMs their climate projection baselines (1961-2000) were compared to the meteorological data observed in the catchment. The seasonal and annual differences between each baseline projection and the observed data were calculated for both, precipitation (%) and mean temperature (%) (Fig. 3). For the mean temperature, BNU-ESM_AN scenario shows the highest difference compared to the observed values as it simulates 1.2% higher temperatures in an annual basis. MPI-ESM-MR_AN fits very well and the results of the other models baseline projections do not differ greatly from the observed data (0.55% as an average). In general, at annual and seasonal scale, the models tend to simulate higher temperatures than those observed, with the exception of summer and especially spring, when some climate projection baselines show lower temperatures than observed ones. Focusing on precipitation, annual projections baselines of CMCC-CESM_SDSM, MPI-ESM-LR_SDSM and MPI-ESM-MR_SDSM are closer to observed precipitation levels (-29%) than other projections, while BNU-ESM_AN and CMCC-CESM_AN show the largest differences with observed (around -50% less precipitation). It is clear that at both annual and seasonal scales the baselines downscaled with the SDSM method fit the observed precipitation better than those downscaled with AN method (Fig. 3). Although the downscaled GCMs chosen were the ones that *a priori* best fitted the observed data provided by AEMET, there are still important differences between the climate projections baselines and the observed meteorological data (especially when precipitation is considered). In order to correct these differences, a linear-scaling approach following the methodology explained by Lenderink et al. (2007) was performed. This approach was selected with a view to altering the downscaled GCMs as little as possible (Graham et al., 2007) without affecting possible trends in future climate projections and derived hydrological projections. Nevertheless, it is important to bear in mind that when the bias correction method is chosen, the selected method will also have associated uncertainties. The approach was applied for all climate projection baselines and future projections in precipitation and maximum and minimum temperature. The bias-corrected values were introduced as meteorological input in SWAT.

2.6. Methodology to evaluate the hydrological impact of the climate projections

For the purpose of studying their hydrological impact, the projections have been divided into three future horizons: 2011-2040, 2041-2070 and 2071-2100, hereafter referred to as the 2030s, 2060s and 2090s, respectively. All future hydrological projections (average discharges) were compared with their baselines at annual and seasonal scales.

Besides that, a study of trends for high and low flow discharge series was made following the methodology described in Zabaleta et al. (2012). To make this analysis, the duration of high and low flows and the severity of low flows were calculated (Hisdal et al., 2001; Wilson et al., 2010) and their trends analyzed. The duration is considered as the period of time (in days) with a discharge value lower than the 0.2 percentile (Q20) for low flows and higher than the 0.8 percentile (Q80) for high flows. Annual and seasonal durations were taken into consideration. The use of Q20 and Q80 percentiles diminishes the weight of extreme maximum and minimum values, which may be subject to measurement error, and provides robustness to the results obtained in the statistical analysis. Severity defines the discharge deficit (volume) below Q20 for low flow and is considered annually. Quantiles, duration, or deficit, have been used by several authors to assess low flows (Smakhtin, 2001; Ouarda et al., 2008).

The Mann-Kendall nonparametric trend test (Mann, 1945; Kendall, 1975) was applied to the series calculated for these two variables. However, the series may show a significant serial correlation; when the serial correlation is positive the Mann-Kendall test tends to overestimate the significance of the trend, whereas when it is negative, the test underestimates the probability of detecting trends. This serial correlation may therefore influence the results of the test (Douglas et al., 2000). To avoid these possible effects, before using the Mann-Kendal test the trend free pre-whitening approach developed by Yue et al. (2002) was applied to the serial data. With the Mann-Kendall test it is possible to identify increasing and decreasing trends and the probability of occurrence (P) of those trends. The value of P can vary between 0 and 1, where 0 indicates that there is no probability of occurrence in the trend and 1 indicates maximum probability. The criteria suggested by the IPCC (Mastrandrea et al., 2010) in its 5th report were used to evaluate P. In this document, likelihood refers to a probabilistic assessment of some well-defined past or future outcomes. The categories defined and used in this research are: P>0.99, virtually certain trend; P>0.95, extremely probable trend; P>0.90, very probable trend and P>0.66, probable trends. Values of P below 0.66 are considered to represent non-probable trends in this work.

3. Results and discussion

3.1. SWAT calibration (1996-2006), validation (2007-2013) and simulation uncertainty

The parameters changed in the calibration process of SWAT for the Upper Nerbioi, their value-range used in the autocalibration and the final values are shown in Table 3. These are some of the most common parameter changes usually performed in SWAT to calibrate the model (Arnold et al., 2012) and all of them were changed taking into account the catchment characteristics. The results of the calibration (1996-2006) and the validation (2007-2013) are displayed in a daily hydrograph with the observed and simulated discharge (Fig. 2). The calibration can be seen to fit the observed data well, although the peak magnitude is underestimated in some high flows. In previous works carried out with the SWAT model (daily time step) in the Basque Country, the underestimation of the peak magnitude is usual (Zabaleta et al., 2014; Peraza et al., 2015; Epelde et al., 2015; Meaurio et al., 2015). This inaccuracy may be related to the inability of the model to properly consider precipitation intensity and spatial-temporal distribution when simulating rapid hydrological responses at the daily time step (Qiu et al., 2012).

In general, simulated discharge peaks fit observed data better during the validation (Fig. 2). The set of statistical indices calculated for daily discharge (Table 4) shows that the model performs satisfactorily during both, calibration and validation (Moriasi et al., 2007).

Analyzing years with a low and high aridity index (AI), it is possible to assess whether the simulation is good enough to make long-term hydrologic projections and evaluate when the greatest uncertainties are found (low or high AI). The set of statistical indices (Table 4) shows that simulation performance for years with high and low AI is at least “good”, although some parameters are slightly poorer for years with high AI (more uncertainty). In addition, the set of statistical indices were also applied for the entire period (1996-2013) on a seasonal scale. It is thus possible to evaluate the model performance considering low (summer), intermediate (spring and autumn) and high (winter) flows and determining where the largest uncertainties are. Winter and spring present "good" statistical results, autumn is "at least satisfactory" and the statistical indices show that although the hydrograph seems not to fit properly in summer (low r^2, NSE and RSR), the water yield is simulated correctly (low PBIAS). Note that summer discharges, being the lowest, are more vulnerable to measurement errors. Therefore, although the simulation does perform well, summer is the season associated to the highest modeling uncertainty. However, according to Moriasi et al. (2007) the values of most of the statistical indices shown in Table 4 were "good" or "very good" at monthly time step. Since these analyses were made with daily values they are considered to be at least "good". Additionally, the p-factor and r-factor obtained with the SWAT-CUP program (the range of the parameters is shown in Table 3) for calibration and validation are 0.81 and 0.41 respectively, which is considered "good" (Abbaspour et al., 2015). As a consequence, it can be said that the performance of the model is good enough for carrying out future hydrological projections with a certain degree of confidence.

3.2. Assessment of the baseline hydrological projections

The bias-corrected precipitation and maximum and minimum temperature for the baseline of each downscaled GCM was introduced in the calibrated and validated SWAT project. The first step was to assess how the hydrological simulations obtained for baseline (1961-2000) adjust to the ones performed using observed meteorological data (OBS_SIM) for the same period. The mean monthly discharges ($m^3 s^{-1}$) obtained are shown in Fig. 4. This figure shows that as in the case of precipitation, hydrological simulations obtained using the baseline climate projections downscaled with the SDSM method fit much better to OBS-SIM than those downscaled with the AN method. In fact, the adjustment for discharge series obtained using SDSM downscaling to OBS_SIM is really good in autumn (-9%) and winter (-2%) whereas in spring and summer the discharge is underestimated by about -22% and -71%, respectively. However, those differences are higher in all seasons for the discharge series obtained using the AN method; around -22% in autumn, -11% in winter, -46% in spring and -83% in summer.

Therefore, it is clear that, in this case, the choice of the downscaling method is the cause of a higher uncertainty source in the obtained discharge series than the choice of the GCM itself.

3.3. Hydrological impact of future climate scenarios: annual and seasonal scales (2011-2100)

To evaluate the impact of climate change on the hydrology of the Upper Nerbioi catchment area, future hydrological projections divided into three time horizons (2030s, 2060s, and 2090s) were compared with their baseline average discharge (1961-2000). The difference in average discharge (in %) is shown in Fig. 5. Focusing on the downscaling method (AN or SDSM), the hydrological projections derived from climate projections that use the AN method always show a smaller discharge decrease than those downscaled with SDSM (with the exception of CMCC_CESM_AN_R85). Considering that climate projections obtained with the SDSM downscaling method fit better to OBS_SIM series data for the baseline period, it seems more reasonable to consider those hydrological projections derived from SDSM downscaled series.

It is also important to compare the two different RCPs because, one would expect that the difference between the 2060s and 2090s for the projections with RCP 4.5 would be minimal, while for 8.5 the difference would continue to increase. Indeed, if the projections of CMCC-CESM are not considered, the difference in discharge at annual scale between the baseline and the projections with RCP 4.5 is -6% for the 2030s, -8% for the 2060s and -9% for the 2090s, while for RCP 8.5 it is -13% for the 2030s; -15% for the 2060s and -20% for the 2090s. In the RCP 4.5 scenario, the seasonal decrease of discharge throughout the century is lower. In some seasons, as in summer, a stabilization of the discharge can be observed, and in others (e.g. autumn) the increase in the average flow in the 2090s almost compensates for the decreases observed during the 2060s. This is not the case for the RCP 8.5 scenario where discharge continues to decrease until the end of the century.

Undeniably CMCC_CESM_AN_R85 is most noteworthy because it projects higher discharge than the baseline. CMCC_CESM_SDSM_R85 decreases respect to the baseline, but as it happens with CMCC_CESM_AN_R85 the discharge increases throughout the century. The results for this GCM were analysed separately due to those different trends shown. Fig. 6 shows the difference (%) between CMCC-CESM_AN_R85 and CMCC-CESM_SDSM_R85 future discharges with regard to their baseline on a seasonal and annual scale. In order to compare not only the trends but also the discharge, in terms of illustrative average flow for each period, the average discharge for each time horizon considered is also displayed in Fig. 6. These are the two projections that simulate highest discharge at annual scale as well as at seasonal scale.

As discussed above, the downscaling method and the selection of RCP have a strong influence on the results. The projections were therefore classified taking into consideration the downscaling method (AN or SDSM) and the scenarios (RCP 4.5 or RCP 8.5) (Fig. 7), analysed in four different groups (with the exception of the CMCC-CESM projections). Thus, the results are an ensemble of projections but it is possible to analyse differences between these factors (downscaling method and RCP). At annual scale, and for the end of the century (2090s), discharge decreases by -9% and -20% for RCP 4.5 and RCP 8.5 scenarios, respectively, with little differences between downscaling methods. These results are consistent with most of the studies carried out in the Atlantic region of France and in the North of the Iberian Peninsula (Table 1). However, focusing on the seasonal changes, significant differences can be found depending on the use of the downscaling method. Summer is the season when the greatest differences can be observed; slightly increasing (<5% for 2090s) for climate projections derived from AN downscaling, and clearly decreasing (-15 to -25% for 2090s) for SDSM-derived ones. The AN downscaling method simulated considerably less discharge than the SDSM downscaling method. Hence, the difference decreases between baseline and future projections are bigger for the SDSM method, although the projections downscaled with SDSM (independent of RCP) always projected more discharge than those downscaled with the AN method (Fig. 7). In other seasons (autumn, winter and spring), discharge decreased regardless of the method chosen, with higher changes when using the AN method in autumn and smaller changes in spring. The results obtained using different downscaling methods are most similar in winter. This is the season that has most weight in the annual discharge, hence its effect can be observed at annual scale. Considering all the models, autumn is the season with the most significant discharge decrease (-17%) followed by spring (-16%), winter (-11%), and summer (-7%) for 2090s. These results are slightly different from previous studies undertaken in the Atlantic region of France and the north of the Iberian Peninsula (Table 1). In most of the research works carried out in these areas the highest discharge decreases occur in summer, and depending on the study are followed by autumn or spring (Table 1). In the present study, considering the average value, summer is not the most affected season in percentage. This could be explained by the influence of the projections downscaled with the AN method (Fig. 7).

Fig. 8 is an ensemble showing a combination of the 16 hydrological projections analysed (average of the mean monthly discharge ($m^3 s^{-1}$) represented in a hydrological year) and their evolution over time measured at the 3 time horizons (2030s, 2060s and 2090s). In order to consider all the discharge predictions obtained, the projections were not divided based on the downscaling method or the RCP. The highest discharge values represent the maximum value of the mean monthly discharge of all of the projections, while the lowest values represent the minimum ones. The possible discharge range is the highest in winter and autumn. In these seasons the possible mean discharge may vary by 4 $m^3 s^{-1}$. In spring the discharge may range between 1 and 2.1 $m^3 s^{-1}$, while the range in summer may be the lowest: between 0.1 and 0.3 $m^3 s^{-1}$. In spring, summer and the beginning of autumn, the projected discharge is always lower than the OBS_SIM. However, the results for spring and summer have to be considered with special care because, as discussed previously, the baseline of the hydrological projections are underestimated and it is therefore probable that a similar phenomenon happens in the case of future projections. With regard to the evolution of the discharge over the century, the projected lowest discharge decreases from the 2030s to the 2090s. The projected highest discharges show the same trend in spring and summer, whereas they may even increase in autumn and winter.

3.4. Evaluation of trends in duration and severity of extreme flows

The results obtained from trend analysis carried out for the duration of extreme flows are shown in Table 5 and Fig. 9. This analysis has been made for the reference period 1961-2000 (Table 5) and the future periods 2011-2040, 2011-2070 and 2011-2100 (Fig. 9). However, the most significant trends appear in the longest period (2011-2100) and hence, these are the results considered in this study.

Analysing the duration (in days) of low flows (<Q20) from 1961 to 2000 (Table 5), the discharge simulated for the reference period (OBS_SIM) does not show any significant annual trend. At seasonal scale, a significant trend is only detected in spring when the low flow duration shows a "probable" upward trend. However, some of the discharge series simulated using the nine climate baselines, show significant trends; an increase at annual scale and, depending on the GCM considered, an increase or decrease in spring, summer and autumn (Table 5).

In the evaluation of future low flow duration (2011-2100; Fig. 9), a general increasing trend can be observed, although, there are a few decreasing trends. In spring and autumn upward trends predominate. In spring the number of projections with significant increasing trends is higher under RCP 8.5 than in RCP 4.5. On the contrary, in autumn this number is lower. Summer present random significant trends mostly under RCP 8.5, that in general tend to be positive. There are few projections with significant trends in winter, therefore, is not possible to obtain clear conclusions for this season.

OBS_SIM displays decreasing annual and seasonal trends for high flow duration (above Q80). Annually, the decreasing trend is "extremely probable", on summer is “very probable” and in autumn, winter and spring is “probable” (Table 5). The high flow durations obtained using climate baselines, in general do not show significant trends. However, the most significant trends are for the model BNU-ESM showing “very probable” to “virtually certain” decreasing trends annually and for autumn.

The high flow duration (Q80) for future projections (2011-2100) show significant trends annually and in autumn, however, there are as many increasing as decreasing trends (Fig. 9). In spring there are few projections with significant trends being most of them increasing. In winter under RCP 8.5 a general decreasing trend predominates. In summer a change in general trend can be observed form RCP 4.5 to RCP 8.5: under RCP 4.5 decreasing trends prevail, while under RCP 8.5 are mostly increasing.

Zabaleta et al. (2012) identified hydrological signs in the catchments of the Basque Country. They used observed daily discharge values in different periods and catchments (regional context). The longest analysed period in their research is 34 years (1973-2007). Although this period does not coincide in time with the reference period used in this work (1961-2000), similarity in the increasing trends of duration of low flows (Q20) can be observed. The authors attributed these trends to hydrological signs of climate change.

Understanding the lower part of the projected hydrographs is essential for an assessment of impact on freshwater ecosystems. Therefore, besides knowing the trend of the number of days with high (above Q80) and low (below Q20) flows, it is also important to know the volumetric deficit (severity) trend, especially for low flows. The OBS_SIM (1961-2000) low flow deficit does not display any significant trend. Most of the baselines do not show significant trends, nevertheless, the few of them where trend is detected, predict an increase in severity.

For 2011-2100 there are significant trends in most of the projected simulations for severity. However, these trends are opposite from each other and cannot be related to the use of given GCMs, downscaling methods or RCP scenarios. As a consequence, severity showed very high uncertainty in future hydrologic projection in the Upper Nerbioi catchment.

4. Conclusions

In this study, to assess future climate change effects (up to year 2100) on the hydrological response of the Upper Nerbioi catchment,16 climate projections combining five GCMs (ACCESS1-0, BNU-ESM, MPI-ESM-RL, MPI-ESM-MR, CMCC-CESM), two downscaling methods (AEMET analogues -AN- and Statistical Downscaling Method -SDSM-) and two Representative Concentration Pathways (RCP 4.5 and RCP 8.5) were considered. Hydrological simulation was performed using the SWAT model achieving satisfactory results for the calibration and validation periods (1996-2013).

Different sources of uncertainties are involved in the hydrologic projections (GCM, downscaling method, RCP, hydrological model). Some conclusions can be drawn from the obtained results even if the quantification of the uncertainties lies outside the scope of this study. The considerable difference between the baselines of the climate models (1961-2000) and the observed meteorological data (the models generally simulate less rainfall, especially in spring and summer) evidences the uncertainty involved for the studied area in the results of the GCMs.

However, downscaling method used resulted in a higher source of uncertainty than GCM itself. When simulated discharges for the baselines of all climate projections were compared with the discharge obtained from a simulation made with the observed meteorological data (OBS_SIM; 1961-2000), the comparison shows that the GCMs downscaled with the SDSM method achieve a much better adjustment than those downscaled with the AEMET analogues (AN). Nevertheless, they all underestimate the discharge amount. Those uncertainties inherent to the methods used at all the levels do not affect the results equally along the year. The seasons with most variable results, and so, the ones for which it is the most difficult to draw a clear conclusion, are spring and especially summer, for which future discharges could either increase or decrease depending on the downscaling method.

From results obtained from four of the analysed GCMs, ACCESS1-0, BNU-ESM, MPI-ESM-RL and MPI-ESM-MR, it can be said that discharge would decrease with respect to the baseline at annual scale. This conclusion is consistent with the trends obtained in the Atlantic region, mostly in France and the Iberian Peninsula (c, d; Table 1). The spatially most homogeneous result from Table 1 is the decrease in summer projections for the entire Atlantic region. However, summer is the season that most discrepancies show in the study area; the projections downscaled with the AN method projected around 5% more discharge for the 2090s than for the baseline whereas SDSM projects -15 to -25% less discharge (Fig 7). In fact, the seasons that predict the largest decrease in discharge in the study area are autumn and spring (around -16 % for 2090s). These downwards trends are also detected in the Atlantic region of France and the Iberian Peninsula, although, they are not so strong. The lowest decrease as it happens in other zones of the Atlantic region, is projected for winter.

For the ensemble of the 16 hydrological projections analysed in the three horizons, the widest range between the monthly highest and lowest discharge values would occur in winter and autumn (around 3-5 $m^3 s^{-1}$) followed by spring (between 0.1-2 $m^3 s^{-1}$) while the narrowest one would be in summer (between 0.1-0.3 $m^3 s^{-1}$). For spring, summer and the beginning of autumn, simulated discharge is always below the

OBS_SIM. In addition, a general decrease on the duration of Q20 is predicted which is a drawback for the achievement of the environmental objectives of the European Water Framework Directive (WFD).

This study was focused in the transition area of the Atlantic region, where climate projections have a high associated uncertainty and the number of research works on hydrological impacts of climate change is scarce (Table 1). The results obtained show the need to consider a wide range of climate projections focusing not only on annual values but also on seasonal variation of discharge. This enables a better approximation of future distribution of freshwater resources. This approximation, together with the consideration of the extremes of the hydrograph in the analysis, highlighted the need to better understand the lower part of the hydrograph, where the related uncertainties are high. This would allow for better planning of future measures in terms of water quantity and quality in catchments of the Atlantic region (Bay of Biscay).

5. Acknowledgements

The authors wish to thank the UPV/EHU (UFI 11/26) and the Basque Government (Consolidated Group IT 598-13) for supporting this research. This study was based on data provided by the Spanish Meteorological Agency (AEMET) of the Spanish Ministry of Environment. The authors also thank Bizkaia Provincial Council and the Basque Meteorological Agency (EUSKALMET) for providing meteorological and discharge data. Maite Meaurio is grateful to the UPV/EHU for financial support within the framework of a PhD grant.

6. References

Abbaspour, K.C., Johnson, C.A., van Genuchten, M.T., 2004. Estimating uncertain flow and transport parameters using a sequential uncertainty fitting procedure. Vadose Zone J. 3 (4), 1340–1352. http://dx.doi.org/10.2113/3.4.1340.

[a]Abbaspour, K.C., Vejdani, M. and Haghighat, S., 2007. SWAT CUP calibration and uncertainty programs for SWAT. International Congress on Modelling and Simulation (MODSIM). 7, 1603-1609.

[b]Abbaspour, K.C., Yang, J., Maximov, I., Siber, R., Bogner, K., Mieleitner, J., Zobrist, J. and Srinivasan, R., 2007. Modelling hydrology and water quality in the pre-alpine/alpine Thur watershed using SWAT. J. Hydrol. 333 (2–4), 413-430. http://dx.doi.org/10.1016/j.jhydrol.2006.09.014.

Abbaspour, K.C., Faramarzi, M., Ghasemi, S.S. and Yang, H., 2009. Assessing the impact of climate change on water resources in Iran. Water Resour. Res. 45, W10434. http://dx.doi.org/10.1029/2008WR007615.

Abbaspour, K.C., Rouholahnejad, E., Vaghefi, S., Srinivasan, R., Yang, H. and Kløve, B., 2015. A continental-scale hydrology and water quality model for Europe: Calibration and uncertainty of a high-resolution large-scale SWAT model. J. Hydrol. 524 (0), 733-752. http://dx.doi.org/10.1016/j.jhydrol.2015.03.027.

Arias, R., 2013. Comportamiento hidrosedimentario de una Cuenca agroforestal bajo diferentes condiciones climáticas: importancia para establecer planes de manejo. PhD, Universidad de Coruña.

Arnell, N.W, 1998. Climate change and water resources in Britain. Clim. Change. 39, 83–110.

Arnell, N.W., 1999. The effect of climate change on hydrological regimes in Europe: A continental perspective. Global Environ. Chang. 9 (1), 5-23. http://dx.doi.org/10.1016/S0959-3780(98)00015-6.

Arnell, N.W., 2004. Climate-change impacts on river flows in Britain: The UKCIPO2 scenarios. Water and Environ. J. 18 (2), 112-117. http://dx.doi.org/10.1111/j.1747-6593.2004.tb00507.x.

Arnell, N.W., 2011. Uncertainty in the relationship between climate forcing and hydrological response in UK catchments. Hydrol. Earth Syst. Sc. 15 (3), 897-912. http://dx.doi.org/10.5194/hess-15-897-2011.

Arnold, J.G. and Allen, P.M.,1996. Estimating hydrologic budgets for three Illinois watersheds. J. Hydrol. 176, 57–77. http://dx.doi.org/10.1016/0022-1694(95)02782-3.

Arnold, J.G., Srinivasan, R., Muttiah, R.S. and Williams, J. R.,1998. Large area hydrologic modeling and assessment – Part 1: model development. J. Am. Water Resour. As. 34 (1), 73–89. http://dx.doi.org/10.1111/j.1752-1688.1998.tb05961.x.

Arnold, J.G., Moriasi, D.N., Gassman, P.W., Abbaspour, K.C., White, M.J., Srinivasan, R., Santhi, C., Harmel, R.D., van Griensven, A., van Liew, M.W., Kannan, N., Jha, M.K., 2012. SWAT: Model use, calibration, and validation. T. ASABE. 55 (4), 1491-1508.

Ayala-Carcedo, F.J. and Iglesias, A., 2000. Impactos del posible cambio climático sobre los recursos hídricos, el diseño y la planificación hidrológica en la España peninsular. El Campo De Las Ciencias y Las Artes. 137, 201-222.

Basque Meteorological Agency: EUSKALMET http://www.euskalmet.euskadi.net

Bastola, S., Murphy, C. and Sweeney, J., 2011. The sensitivity of fluvial flood risk in Irish catchments to the range of IPCC AR4 climate change scenarios. Sci. Total Environ. 409 (24), 5403-5415. http://dx.doi.org/10.1016/j.scitotenv.2011.08.042.

Bates, B.C., Kundzewicz, Z.W., Wu, S. and Palutikof, J.P., 2008. Climate Change and Water, Technical Paper of the Intergovernmental Panel for Climate Change. IPCC. http://www.ipcc.ch/pdf/technical-papers/climate-change-water-en.pdf.. Accessed 5 August 2015.

Bekele, E.G. and Knapp, H.V., 2010. Watershed modeling to assessing impacts of potential climate change on water supply availability. Water Resour. Manag. 24 (13), 3299-3320. http://dx.doi.org/10.1007/s11269-010-9607-y.

Bender, E.A., Case, T.J. and Gilpin, M.E., 1984. Perturbation Experiments in Community Ecology: Theory and Practice. Ecology 65, 1–13. http://dx.doi.org/10.2307/1939452.

Bergstrom, S., Carlsson, B., Gardelin, M., Lindstro, G., Pettersson, A., Rummukainen, M., 2001. Climate change impacts on runoff in Sweden: assessments by global climate models, dynamical downscaling and hydrological modelling. Clim. Res. 16, 101–112.

Boé, J., Terray, L., Martin, E. and Habets, F., 2009. Projected changes in components of the hydrological cycle in French river basins during the 21st century. Water Resour. Res. 45, W08426. http://dx.doi.org.10.1029/2008WR007437.

Boorman, D.B. and Sefton, C.E.M., 1997. Recognizing the uncertainty in the quantification of the effects of climate change on hydrological response. Climatic Change. 35 (4), 415–434.

Bouraoui, F., Galbiati, L. and Bidoglio, G., 2002. Climate change impacts on nutrient loads in the Yorkshire Ouse catchment (U.K.). Hydrol. Earth Syst. Sc. 6 (2), 197-209.

Boyer, C., Chaumont, D., Chartier, I. and Roy, A.G., 2010. Impact of climate change on the hydrology of St. Lawrence tributaries. J. Hydrol. 384, 65-83. http://dx.doi.org/10.1016/j.jhydrol.2010.01.011.

Brands, S., Herrera, S., San-Martin, D. and Gutierrez, J.M., 2011. Validation of the ENSEMBLES global climate models over southwester Europe using probability density functions, from a downscaling perspective. Clim. Res. 48 (2-3), 145-161. http://dx.doi.org/10.3354/cr00995.

Brauman, K.A., Daily, G.C., Duarte, T.K. and Mooney, H.A., 2007. The Nature and Value of Ecosystem Services: An Overview Highlighting Hydrologic Services. Annu. Rev. Environ. Resour., 32, 67–98. http://dx.doi.org/10.1146/annurev.energy.32.031306.102758.

Brigode, P., Oudin, L., and Perrin, C., 2013. Hydrological model parameter instability: A source of additional uncertainty in estimating the hydrological impacts of climate change? J. Hydrol. 476 (0), 410-425. http://dx.doi.org/10.1016/j.jhydrol.2012.11.012.

Brunet, B., Casado, M.J., de Castro, M., Galán, P., López, J.A., Martín, J.M., Pastor, A., Petisco, E., Ramos, P., Ribalaygua, J., Rodríguez, E., Sanz, I. Torres, L., 2009. Generación de Escenarios Regionalizados de Cambio Climático para España. Spanish Meteorological Agency (AEMET).http://www.aemet.es/documentos/es/serviciosclimaticos/cambio_climat/datos_diarios/Informe_Escenarios.pdf.Accessed 5 August 2015.

Caballero, Y., Voirin-Morel, S., Habets, F., Noilhan, J., LeMoigne, P., Lehenaff, A. and Boone, A., 2007. Hydrological sensitivity of the Adour-Garonne river basin to climate change. Water Resour. Res. 43 (7), W07448. http://dx.doi.org/10.1029/2005WR004192.

Carvalho-Santos, C., Nunes, J.P., Monteiro, A.T., Hein, L. and Honrado, J.P., 2015. Assessing the effects of land cover and future climate conditions on the provision of hydrological services in a medium-sized watershed of Portugal. Hydrol. Process. n/a-n/a. http://dx.doi.org/10.1002/hyp.10621

CEDEX (Centro de Estudios y Experimentación de Obras Públicas) 2010. Necesidades de adaptación al cambio climático de la red troncal de infraestructuras de transporte en España. Informe final. http://www.adaptecca.es/sites/default/files/editor_documentos/accit_informe_final_septiembre_2013.pdf. Accessed 5 August 2015.

Charlton, M.B., and Arnell, N.W., 2014. Assessing the impacts of climate change on river flows in England using the UKCP09 climate change projections. J. Hydrol. 519, Part B, 1723-1738. http://dx.doi.org/10.1016/j.jhydrol.2014.09.008.

Chauveau, M., Chazot, S., Perrin, C., Bourgin, P., Sauquet, E., Vidal, J., Rouchy, N., Martin, E., David, J., Norotte, T., Maugis, P. and de Lacaze, X., 2013. What will be the impacts of climate change on surface hydrology in France by 2070? La Houille Blanche-Revue Internationale De L´Eau. (4), 5-15. http://dx.doi.org/10.1051/lhb/2013027.

Chen, J., Brissette, F.P. and Leonte, R., 2011. Uncertainty of downscaling method in quantifying the impact of climate change on hydrology. J. Hydrol. 40,190-202. http://dx.doi.org/10.1016/j.jhydrol.2011.02.020.

Chow, V.T., Maidment, D.R. and Mays, L.W., 1988.Applied Hydrology. McGraw-Hill Inc, New York, USA.

Cloke, H. L., Jeffers, C., Wetterhall, F., Byrne, T., Lowe, J., and Pappenberger, F., 2010. Climate impacts on river flow: Projections for the medway catchment, UK, with UKCP09 and CATCHMOD. Hydrol. Process. 24 (24), 3476-3489. http://dx.doi.org.10.1002/hyp.7769.

Coch, A. and Mediero, L., 2015. Trends in low flows in Spain in the period 1949–2009. Hydrolog. Sci. J. 1-17. http://dx.doi.org//10.1080/02626667.2015.1081202.

Da Cunha, L.V., De Oliveira, R.P., Nascimento, J., and Ribeiro, L., 2007. Impacts of climate change on water resources: A case-study for Portugal. Water in Celtic Countries: Quantity, Quality and Climate Variability, 310, 37-48.

Diaz-Nieto, J. and Wilby, R.L., 2005. A comparison of statistical downscaling and climate change factor methods: Impacts on low flows in the river Thames, United Kingdom. Climatic Change. 69 (2), 245-268.

Dibike, Y.B. and Coulibaly, P., 2005. Hydrologic impact of climate change in the Saguenay watershed: comparison of downscaling methods and hydrologic models. J. Hydrlk, 307 (1–4), 145-163. http://doi.org/10.1016/j.jhydrol.2004.10.012.

Douglas, E.M., Voguel, R.M. and Kroll, C.N., 2000. Trends in floods and low flows in the United States: Impact of spatial correlation. J. Hydrol. 240, 90–105. http://dx.doi.org/10.1016/S0022-1694(00)00336-X.

Ducharne, A., Habets, F., Page, C., Sauquet, E., Viennot, P., Deque, M., Gascoin, S., Hachour, A., Martin, E., Oudin, L., Terray, L. and Thiery, D., 2010. Climate change impacts on water resources and hydrological extremes in northern France. Proceedings of the XVIII International Conference on Computational Methods in Water Resources (Cmwr 2010), 243-250.

Epelde, A.M., Cerro, I., Sanchez-Perez, J.M., Sauvage, S., Srinivasan, R., and Antigueedad, I., 2015. Application of the SWAT model to assess the impact of changes in agricultural management practices on water quality. Hydrol. Sci. J. 60 (5), 825-843. http://dx.doi.org/10.1080/02626667.2014.967692.

FAO, 1977. Guidelines for Soil Profile Description. Rome, Italy.

Fowler, H.J. and Kilsby, C.G., 2007. Using regional climate model data to simulate historical and future river flows in northwest England. Climatic Change. 80 (3-4), 337-367. http://dx.doi.org/10.1007/s10584-006-9117-3.

Fowler, H.J., Blenkinsop, S. and Tebaldi, C., 2007. Linking climate change modelling to impacts studies: recent advances in downscaling techniques for hydrological modelling. Int. J. Climatol. 27 (12), 1547–1578. http://dx.doi.org/10.1002/joc.1556.

Geographical data base of the Basque Government, GEOEUSKADI; http://www.geo.euskadi.net

Giorgi, F. and Mearns, L.O., 2002. Calculation of average, uncertainty range, and reliability of regional climate changes from AOGCM simulations via the ‘‘reliability ensemble averaging’’ (REA) method. J. Climate. 15, 1141–1158. http://dx.doi.org/10.1175/1520-0442(2003)016%3C0883:COCOAU%3E2.0.CO;2.

Görgen, K., Beersma, J., Brahmer, G., Buiteveld, H., Carambia, M., de Keizer, O., Krahe, P., Nilson, E., Lammersen, R., Perrin, C. and Volken, D., 2010. Assessment of

Climate Change Impacts on Discharge in the Rhine River Basin: Results of the RheinBlick2050 Project, CHR Report, 1–23, 229 pp, Lelystad, ISBN 978-90-70980-35-1.

Gosling, S.N., Taylor, R.G., Arnell, N.W. and Todd, M.C., 2011. A comparative analysis of projected impacts of climate change on river runoff from global and catchment-scale hydrological models. Hydrol. Earth. Syst. Sc. 15, 279-294. http://dx.doi.org/10.5194/hess-15-279-2011.

Goubanova, K. and Li, L., 2007. Extremes in temperature and precipitation around the Mediterranean basin in an ensemble of future climate scenario simulations. Glob. Planet. Chang. 57, 27–42

Graham, L.P., Andréasson, J. and Carlsson, B., 2007. Assessing climate change impacts on hydrology from an ensemble of regional climate models, model scales and linking methods – a case study on the Lule River Basin. Climatic Change. 81 (1), 293-307. http://dx.doi.org/10.1007/s10584-006-9215-2.

Green, W.H. and Ampt, G.A., 1911. Studies on soil physics. The Journal of Agricultural Science. 4 (1), 1-24. http://dx.doi.org/10.1017/S0021859600001441.

Gupta, H.V., Sorooshian, S. and Yapo, P.O., 1999. Status of automatic calibration for hydrologic models: Comparison with multilevel expert calibration. J. Hydrol.Eng. 4 (2), 135-143.

Habets, F., Boe, J., Deque, M., Ducharne, A., Gascoin, S., Hachour, A., Martin, E., Page, C., Sauquet, E., Terray, L., Thiery, D., Oudin, L. and Viennot, P., 2013. Impact of climate change on the hydrogeology of two basins in northern France. Climatic Change. 121 (4), 771-785. http://dx.doi.org/10.1007/s10584-013-0934-x.

Hargreaves, G. and Samani, Z.A., 1985. Reference crop evapotranspiration from temperature. Appl. Eng. Agric. 1 (2), 96-99. http://dx.doi.org/10.13031/2013.26773.

Hewitson, B.C. and Crane, R.G., 1996. Climate downscaling: techniques and application. Clim. Res. 7, 85-95.

Hiscock, K., Sparkes, R., and Hodgson, A., 2011. Evaluation of future climate change impacts on European groundwater resources. Climate Change Effects on Groundwater Resources: A Global Synthesis of Findings and Recommendations. 27, 351-365.

Hisdal, H., Stahl, K., Tallaksen, L.M. and Demuth, S., 2001. Have streamflow droughts in Europe become more severe or frequent? Int. J. Climatol. 21, 317–333. http://dxdoi.org/10.1002/joc.619.

Iñiguez, J., Sánchez-Carpintero, I., Val, R.M., Romeo, A. and Basconesm, J.C., 1980. Mapa de suelos de Alava. Vitoria-Gasteiz: Diputación Foral de Alava-Departamento de Edafología de la Universidad de Navarra.

IPCC, 2007. Climate Change 2007: synthesis report. Contribution of working groups I, II and III to the Fourth Assessment Report of the Intergovernmental Panel on Climate Change. Core Writing Team, R.K. Pachauri, and A. Reisinger, eds. Geneva: IPCC Secretariat.

IPCC, 2013. Climate Change 2013: The Physical Science Basis. Contribution of Working Group I to the Fifth Assessment Report of the Intergovernmental Panel on Climate Change. [Stocker, T.F., D. Qin, G.-K. Plattner, M. Tignor, S.K. Allen, J. Boschung, A. Nauels, Y. Xia, V. Bex and P.M. Midgley (eds.)]. Cambridge University Press, Cambridge, United Kingdom and New York, NY, USA, 1535pJohnson, F. and Sharma, A., 2009. Measurement of GCM skill in predicting variables relevant for hydroclimatological assessments. J. Climate. 22 (16), 4373-4328. http://doi.org/10.1175/2009JCLI2681.1.

Jothityangkoon, C., Sivapalan, M. and Farmer, D.L., 2001. Process controls of water balance variability in a large semi-arid catchment: downward approach to hydrological model development. J. Hydro. 254,174–198. http://dx.doi.org/10.1016/S0022-1694(01)00496-6.

Kay, A.L., Davies, H.N., Bell, V.A. and Jones, R.G., 2009. Comparison of uncertainty sources for climate change impacts: flood frequency in England. Climatic Change. 92, 41-63. http://dx.doi.org/10.1007/s10584-008-9471-4.

Kay, A.L., Jones, R.G. and Reynard, N.S., 2006. RCM rainfall for UK flood frequency estimation II. Climate change results. J. Hydrol. 318, 163-172. http://dx.doi.org/10.1016/j.jhydrol.2005.06.013.

Kendall, M.G., 1975. Rank correlation measures. Charles Griffin, London, UK.

Kiely, G., 1999. Climate change in Ireland from precipitation and streamflow observation. Adv. Water. Resour. 23, 141–151.

Lahmer, W., Pfutzner, B. and Becker, A., 2001. Assessment of land use and climate change impacts on the mesoscale. Physics and Chemistry of the Earth, Part B. Hydrol. Ocean. Atmos., 26 (7–8), 565–575. http://dx.doi.org/10.1016/S1464-1909(01)00051-X.

Leavesley, G.H., 1994.Modeling the effects of climate change on water resources – a review. Climatic Change. 28, 159–177.

Lenderink, G., Buishand, A. and van Deursen, W., 2007. Estimates of future discharges of the river Rhine using two scenario methodologies: direct versus delta approach. Hydrol. Earth Syst. Sc. 11 (3), 1145–1159. http://dx.doi.org/10.5194/hess-11-1145-2007.

Lespinas, F., Ludwig, W. and Heussner, S., 2014. Hydrological and climatic uncertainties associated with modeling the impact of climate change on water resources of small Mediterranean coastal rivers. J. Hydrol. 511, 403 – 422. http://dx.doi.org/10.1016/j.jhydrol.2014.01.033.

Li, Z., Liu, W., Zhang, X. and Zheng, F., 2009. Impacts of land use change and climate variability on hydrology in an agricultural catchment on the Loess Plateau of China. J. Hydrol. 377, 35-42. http://dx.doi.org/10.1016/j.jhydrol.2009.08.007.

Mann, H.B., 1945. Non-Parametric tests against trend. The Econometric Society. 13, 245–259. http://dx.doi.org/10.2307/1907187.

Maraun, D., Wetterhall, F., Ireson, A.M., Chandler, R.E., 2010. Precipitation downscaling under climate change. Recent developments to bridge the gap between dynamical models and the end user. Rev. Geophys. 48 (3), 1944-9208. http://dx.doi.org/10.1029/2009RG000314.

Mastrandrea, M.D., Field, C.B., Stocker, T.F., Edenhofer, O., Ebi, K.L., Frame, D.J., Held, H., Kriegler, E., Mach, K.J., Matschoss, P.R., Plattner, G-K., Yohe, G.W. and Zwiers, F.W., 2010. Guidance Note for Lead Authors of the IPCC Fifth Assessment Report on Consistent Treatment of Uncertainties. Intergovernmental Panel on Climate Change (IPCC). Available in http://www.ipcc.ch. Accessed 5 August 2015.

Meaurio, M., Zabaleta, A., Uriarte, J.A., Srinivasan, R. and Antigüedad, I., 2015. Evaluation of SWAT models performance to simulate streamflow spatial origin. The case of a small forested watershed. J. Hydrol. 525, 326-334. http://dx.doi.org/10.1016/j.jhydrol.2015.03.050.

Mediero, L., Kjeldsen, T.R., Macdonald, N., Kohnova, S., Merz, B., Vorogushyn, S., Wilson, D., Alburquerque, T., Bloeschl, G., Bogdanowicz, E., Castellarin, A., Hall, J., Kobold, M., Kriauciuniene, J., Lang, M., Madsen, H., Gul, G.O., Perdigao, R.A.P., Roald, L.A., Salinas, J.L., Toumazis, A.D., Veijalainen, N. and Porarinsson, O., 2015. Identification of coherent flood regions across Europe by using the longest streamflow records. J. Hydrol.. 528, 341-360. http://.dx.doi.org/10.1016/j.jhydrol.2015.06.016.

Meinshausen, M., Smith, S.J., Calvin, K., Daniel, J.S., Kainuma, M.L.T., Lamarque, J-F., Matsumoto, K., Montzka, S.A., Raper, S.C.B., Riahi, K., Thomson, A., Velders, G.J.M. and van Vuuren, D.P.P., 2011. The RCP greenhouse gas concentrations and their extensions from 1765 to 2300. Climatic Change. 109 (1-2), 213-241. http://dx.doi.org/10.1007/s10584-011-0156-z.

Mimikou, M.A., Baltas, E., Varanou, E., Pantazis, K., 2000. Regional impacts of climate change on water resources quantity and quality indicators. J. Hydrol. 234, 95–109.

Monteith, J.L., 1965. Evaporation and environment: the state and movement of water in living organisms. Symposia of the Society for Experimental Biology.19, 205–234.

Moriasi, D.N., Arnold, J.G., Van Liew, M.W., Bingner, R.L., Harmel, R.D. and Veith, T.L., 2007. Model evaluation guidelines for systematic quantification of accuracy in watershed simulations. Watershed Simulations. T. ASABE. 50 (3), 885–900.

Moss, R. H., Edmonds, J.A., Hibbard, K.A., Manning, M.R., Rose, S.K., van Vuuren, D.P., Carter, T.R., Emori, S., Kainuma, M., Kram, T., Meehl, G.A., Mitchell, J.F.B., Nakicenovic, N., Riahi, K., Smith, S.J., Stouffer, R.J., Thomson, A.M., Weyant, J.P. and Wilbanks, T.J., 2010. The next generation of scenarios for climate change research and assessment. Nature. 463 (7282), 747-756. http://dx.doi.org/10.1038/nature08823.

Murphy, J.M., Sexton, D.M.H., Barnett, D.N., Jones, G.S., Webb, M.J. and Stainforth, D.A., 2004. Quantification of modelling uncertainties in a large ensemble of climate change simulations. Nature, 430, 768–772. http://dx.doi.org/10.1038/nature02771.

Nash, J.E. and Sutcliffe, J.V., 1970. River flow forecasting through conceptual models: Part 1. A discussion of principles. J. Hydrol.10 (3), 282-290. http://dx.doi.org/10.1016/0022-1694(70)90255-6.

Nijssen, B., O'donnell, G.M., Hamlet, A.F. and Lettenmaier, D.P., 2001. Hydrologic sensitivity of global rivers to climate change. Clim. Chang. 50, 143–175.

Ouarda, T.B.M.J., Charron, C. and St-Hilaire, A., 2008. Statistical models and the estimation of low flows. Can. Water Resour. J. 33 (2), 195-206. http://dx.doi.org/10.4296/cwrj3302195.

Overton, D.E., 1966. Muskingum flood routing of upland streamflow. J. Hydrol. 4, 185-200. http://dx.doi.org/10.1016/0022-1694(66)90079-5.

Peraza-Castro, M., Ruiz-Romera, E., Montoya-Armenta, L.H., Sanchez-Perez, J.M. and Sauvage, S., 2015. Evaluation of hydrology, suspended sediment and nickel loads in a small watershed in Basque Country (northern Spain) using eco-hydrological SWAT model. Ann. Limnol-Int. J. Lim. 51 (1), 59-70. http://dx.doi.org/10.1051/limn/2015006.

Perez, J., Menendez, M., Mendez, F. and Losada, I., 2014. Evaluating the performance of CMIP3 and CMIP5 global climate models over the north-east Atlantic region. Clim. Dynam. 43 (9-10), 2663-2680. http://dx.doi.org/10.1007/s00382-014-2078-8.

Petisco, S.E. and Martín, J.M., 2006. Escenarios de temperatura y precipitación para la España peninsular y Baleares durante el período 2001-2100 basados en “downscaling” estadístico mediante métodos de análogos. XXIX Jornadas Científicas de la Asociación Meteorológica Española. Pamplona.

Priestley, C.H.B. and Taylor, R.J., 1972. On the assessment of surface heat flux and evaporation using large-scale parameters. Monthly Weather Review,100, 81–92.

Prudhomme, C., Young, A., Watts, G., Haxton, T., Crooks, S., Williamson, J., Davies, H., Dadson, S. and Allen, S., 2012. The drying up of Britain? A national estimate of changes in seasonal river flows from 11 regional climate model simulations. Hydrological Processes. 26 (7), 1115-1118. http://dx.doi.org/10.1002/hyp.8434.

Qiu, L.J., Zheng, F.L. and Yin, R.S., 2012. SWAT-based runoff and sediment simulation in a small watershed, the loessial hilly-gullied region of China: Capabilities and challenges. Int. J. Sediment Res. 27:226–234. http://dx.doi.org/10.1016/S1001-6279(12)60030-4.

Ribalaygua, J., Pino, M.R., Pórtoles, J., Roldán, E., Gaitán, E., Chinarro, D. and Torres, L., 2013. Climate change scenarios for temperature and precipitation in Aragón (Spain). Sci. Total Environ. 463–464 (0), 1015-1030. http://dx.doi.org/10.1016/j.scitotenv.2013.06.089.

Shorthouse, C. and Arnell, N., 1999. The effects of climate variability on spatial characteristics of European river flows. Phys. Chem. Earth 24 (1–2), 7–13.

Sloan, P.G. and Moore, I.D., 1984. Modeling surface and subsurface stormflow on steeply sloping forested watersheds. Water Resour. Res. 20 (12), 1815-1822. http://dx.doi.org/10.1029/WR020i012p01815.

Smakhtin, V.Y., 2001. Low flow hydrology: a review. J. Hydrol. 240, 147-186. http://dx.doi.org/10.1016/S0022-1694(00)00340-1.

Stahl, K., Tallaksen, L.M., Gudmundsson, L. and Christensen, J.H.,2011. Streamflow data from small basins: a challenging test to high resolution regional climate modeling, J. Hydrometeorol. 12, 900–912.

Steele-Dunne, S., Lynch, P., McGrath, R., Semmler, T., Wang, S., Hanafin, J. and Nolan, P., 2008. The impacts of climate change on hydrology in Ireland. J. Hydrol. 356 (1-2), 28-45. http://dx.doi.org/10.1016/j.jhydrol.2008.03.025.

Szêpszô, G., Lingemann, I., Klein, B., and Kovacs, M., 2014. Impact of climate change on hydrological conditions of Rhine and upper Danube rivers based on the results of regional climate and hydrological models. Nat. Hazards. 72 (1), 241-262. Http://dx.doi.org/10.1007/s11069-013-0987-1.

Tavakoli, M., De Smedt, F., Vansteenkiste, T., and Willems, P., 2014. Impact of climate change and urban development on extreme flows in the Grote Nete watershed, Belgium. Nat. Hazards. 71(3), 2127-2142. http://dx.doi.org//10.1007/s11069-013-1001-7.

Taylor, K. E., Stouffer, R. J. and Meehl, G. A., 2012. An overview of CMIP5 and the experiment design. American Meteorological Society. 93, 485-498. doi:10.1175/BAMS-D-11-00094.1.

Teng, J., Vaze, J., Chiew, F.H.S., Wang, B. and Perraud, J.M., 2012. Estimating the relative uncertainties sourced from GCMs and hydrological models in modeling climate change impact on runoff. J. Hydrometeorol. 13 (1), 122–139. http://dx.doi.org/10.1175/JHM-D-11-058.1.

Touhami, I., Chirino, E., Andreu, J.M., Sánchez, J.R., Moutahir, H. and Bellot, J., 2015. Assessment of climate change impacts on soil water balance and aquifer recharge in a semiarid region in south east Spain. J. Hydrol. 527 (0), 619-629. http://dx.doi.org/10.1016/j.jhydrol.2015.05.012.

USDA Soil Conservation Service, 1972. National Engineering Handbook. Hydrology Section 4 (Chapters 4–10).

Valverde, P., Serralheiro, R., de Carvalho, M., Maia, R., Oliveira, B. and Ramos, V., 2015. Climate change impacts on irrigated agriculture in the Guadiana river basin (Portugal). Agr. Water Manage. 152 (0), 17-30. http://dx.doi.org/10.1016/j.agwat.2014.12.012.

van Griensven, A., Meixner, T. and Grunwald. S., 2006.A global sensitivity analysis tool for the parameters of multi-variable catchment models. J. Hydrol. 324, 10-23. http://dx.doi.org/10.1016/j.jhydrol.2005.09.008.

van Vuuren, D. P., Edmonds, J., Kainuma, M., Riahi, K., Thomson, A., Hibbard, K., Hurtt, G.C., Kram, T., Krey, V., Lamarque, J., Masui, T., Meinshausen, M., Nakicenovic, N., Smith, S.J. and Rose, S.K., 2011. The representative concentration pathways: An overview. Climatic Change. 109(1-2), 5-31. http://dx.doi.org/10.1007/s10584-011-0148-z.

Vörösmarty, C.J., McIntyre, P.B., Gessner, M.O., Dudgeon, D., Prusevich, A., Green, P., Glidden, S., Bunn, S.E., Sullivan, C.A., Liermann, C.R. and Davies, P.M., 2010. Global threats to human water security and river biodiversity. Nature, 467 (7315), 555-561. http://dx.doi.org/10.1038/nature09440.

Wilby R.L., Orr, H.G., Hedger, M., Forrow, D. and Blackmore, M., 2006. Risk posed by climate change to the delivery of Water Framework Directive objectives in the UK. Environ. Int. 32, 1043-1055. http://doi.org.10.1016/j.envint.2006.06.017.

Wilby, R.L. and Harris, I., 2006. A framework for assessing uncertainties in climate change impacts: low-flow scenarios for the River Thames, UK. Water Resour. Res. 42 (2), 1944-7973. http://doi.org/10.1029/2005WR004065.

Wilby, R.L. and Wigley, T.M.L., 1997. Downscaling general circulation model output: a review of methods and limitations. Prog. Phys. Geog. 21, 530-548. http://dx.doi.org/10.1177/030913339702100403.

Wilby, R.L., 2005. Uncertainty in water resource model parameters used for climate change impact assessment. Hydrol. Process. 19 (16), 3201–3219. http://doi.org/10.1002/hyp.5819.

Wilby, R.L., Dawson, C.W. and Barrow, E.M., 2002. SDSM-A decision support tool for the assessment of regional climate change impacts. Environ. Modell. Softw. 17, 145-157. http://dx.doi.org/10.1016/S1364-8152(01)00060-3.

Williams, J.R., 1969. Flood routing with variable travel time or variable storage coefficients. T. ASABE. 12 (1): 0100-0103. http://dx.doi.org/10.13031/2013.38772.

Wilson, D., Hisdal, D. and Lawrence, D., 2010. Has streamflow changed in the Nordic countries? – Recent trends and comparisons to hydrological projections. J. Hydrol. 394, 334-346. http://dx.doi.org/10.1016/j.jhydrol.2010.09.010.

Xu, C.Y., Halldin, S., 1997. The effect of climate change on river flow and snow cover in the NOPEX area simulated by a single water balance model. Nordic Hydrol. 28, 273–282.

Yue, S., Pilon, P., Phinney, B. and Cavadias, G., 2002. The influence of autocorrelation on the ability to detect trend in hydrological series. Hydrol. Process. 16, 1807– 1829. http://dx.doi.org710.1002/hyp.1095.

Zabaleta, A., Meaurio, M., Ruiz, E. and Antigüedad, I., 2014. Simulation climate change impact on runoff and sediment yield in a small watershed in the Basque Country, northern Spain. J. Environ. Qual. 43, 235–245. http://dx.doi.org/10.2134/jeq2012.0209.

Zabaleta, A., Morales, T., Meaurio, M., Gorria, C. and Antigüedad, I., 2012. Regional hydrological signs for climate change in Southern Europe (Basque Country). International Conference on Water. Climate and Environment. ISBN 978-608-4510-10-9.

Zhang, X., Xu Y. and Fu, G., 2014. Uncertainties in SWAT extreme flow simulation under climate change. J. Hydrol. 515 (0), 205-222. http://dx.doi.org/10.1016/j.jhydrol.2014.04.064.

Zorita, E. and von Storch, H.,1999. The analog method as a simple statistical downscaling technique: comparison with more complicated methods. J. Climate. 12, 2474-2.

Table 1. Summary of research works carried out in the Atlantic region (IPCC, 2007) on the hydrological impact of climate change considering the following information: Work reference (Ref.), location, climatic model, hydrological model (Hydro. Model), Downscaling method (Down.) and Scenario (Scen.). “D” stands for Dynamic, “S” Static, “pf” peak flow and “lf” low flow. Results are given in % of the discharge variation with regard to the discharge simulated for the baseline in annual and seasonal basis for the decades of the 40s, 70s and 100s. References: (a) Belgium and Netherlands; (b) United Kingdom; (c) France; (d) Iberian Peninsula; 1: Szêpszô et al., 2014; 2: Tavakoli et al., 2014; 3: Arnell, 2004; 4: Diaz-Nieto and Wilby, 2005; 5: Fowler and Kilsby, 2007; 6: Steele-Dunne et al., 2008; 7: Cloke et al., 2010; 8: Arnell, 2011; 9: Bastola et al., 2011; 10: Prudhomme et al., 2012; 11: Charlton and Arnell., 2014; 12: Caballero et al., 2007; 13: Boé et al., 2009; 14: Ducharne et al., 2010; 15: Chauveau et al., 2013; 16: Habets et al., 2013; 17: Da Cunha et al., 2007; 18: CEDEX 2010; 19: Arias, 2013; 20: Carvalho-Santos et al., 2015.

REF.	LOCATION	CLIMATIC MODEL	HYDRO. MODEL	DOWN.	SCEN.	ANNUAL			AUTUMN			WINTER			SPRING			SUMMER		
						40	70	100	40	70	100	40	70	100	40	70	100	40	70	100
1 (a)	Rhine and Upper Danube	ECCONET EU FP7, CMIP3	HBV134, COSERO	D	A1B				↑			↑10- ↓10						0-↓20		
2 (a)	Grote Nete Belgium	CCI-HYDR	WetSpa	S	High, med. & low		↑75pf ↓4.7lf													
3 (b)	Britain	UKCIP02.	-	-	A2	↑10						↑						↓30		
4 (b)	Thames, England	UKCIP02. HadRM3H	CATCHMOD	S	A2	↓7	↓8	↓3	↓8	↓22	↓14	↓1	↓5	↑21	↓12	↓1	↓11	↓6	↓6	↓7
					B2	↑21	↓6	↓3	↑10	↓22	↓20	↑11	↑12	↑12	↑3	↓7	-	↑11	↓7	↓3
5 (b)	8 in NW England	UKCIP02. HadRM3H	ADM	D	A2	↓4	↓10	↓16	↓2	↓1	↓1	↑6	↑11	↑15	↓7	↓15	↓25	↓15	↓34	↓54
6 (b)	9 Irish catchments	ECHAM5	HBV-Light	D	A1B		↑20- ↓20			↑20- ↓5			↑10- ↓40			↑10- ↓50			↓20- ↓65	
7 (b)	Medway, England	UKCP09 HadRM3	CATCHMOD	D	A1B				↓5- ↓15	↑10- ↓20	↑10- ↓30	↓10- ↓20	↓20- ↓30	↓38- ↓50	↓5- ↓20	↓20- ↓35	↓40- ↓50	↓5- ↓15	↓20- ↓30	↓50- ↓55
8(b)	6 in UK	QUEST-GSI CMIP3	Cat-PDM	S	↑2°C														↑20- ↓40	
9(b)	4 Irish	CMIP3	TOPMODEL, NAM, HYMOD	-	A2 B2	↓3	↓9	↓8	↓1	↑1	↑3	↑1	↓3	↓3	-	↓15	↓13	↓14	↓20	↓19
10(b)	UK	UKCP09 HadRM3	CERF	D	A1B					↑60- ↓80			↑40- ↓20			↓40			↑20- ↓80	
11(b)	6 in England	UKCP09	Cat-PDM	S & D	B1 A1B A1FI	↑15- ↓25	↑15- ↓38	↑20- ↓40												
12(c)	Adour-Garonne	CMIP2	SAFRAN-ISBA-MODCOU (SIM)	D	B2					↓			↑			↓			↓11	
13(c)	W France	CMIP3	SAFRAN-ISBA-MODCOU (SIM)	S			↓20			↓30			↓20			↓30			↓30	
14(c)	Seine and Somme, France	RExHySS SAFRAN	MODCOU, SIM, CLSM, EROS / GARDENIA, GR4J	S & D			↓28													
15(c)	NW France	RExHySS CMIP3	Isba-Modcou, GR4J	S	A1B		↓10- ↓60			↓			↓			↓			↓	
16(c)	Seine and Somme, France	RExHySS CMIP3	CLSM, EROS, GARDENIA, GR4, MARTHE, MODCOU, SIM	S & D	A1B A2		↓20	↓30					0	↓15					↓30	↓40
17 (d)	North Douro,	HadCM3	TEMEZ	-	323 ppmv CO_2	↓10	↓20		↓10	↓35		↑20			↓17	↓22		↓30		
		HadRM2		D				↑20			↓35			↑37						↓65
18(d)	Cantabrian region	IPCC, AR3	SIMPA	S & D	A2	↓13	↓16	↓29	↓10			↓10			↓12			↓34		
					B2	↓10	↓16	↓17	↓8			↓4			↓11			↓35		
19 (d)	NW Iberian Peninsula	ENSEMBLES	SWAT	-	A1B					↓10- ↓25	↓10- ↓25		↓10- ↓30	↓5- ↓20		↓10- ↓30	↓15- ↓35		↓18- ↓35	↓15- ↓38
20 (d)	Vez (Portugal)	CMIP5	SWAT	S	RCP 4.5	↓6	↓13		0	↓6		↑2	↑3		↓9	↓614		↓17	↓35	

Table 2. Overview of the General Circulation Models (GCMs) used in the present study, the institution in which they were developed, the country, the downscaling methods used for each GCM, the Representative Concentration Pathway (RCP) and the name given to each climate projection (2011-2100). Note that the name of the baseline projections (1961-2000) follows the same system but without an RCP.

GCM name	Institution	Country	Downscaling method	RCP	Climatic projection name
ACCESS1-0	CSIRO-BOM	Australia	AEMET analog	4.5	ACCESS1-0_AN_R45
				8.5	ACCESS1-0_AN_R85
BNU-ESM	College of Global Change and Earth System Science	China	AEMET analog	4.5	BNU-ESM_AN_R45
				8.5	BNU-ESM_AN_R85
			SDSM	4.5	BNU-ESM_SDSM_R45
				8.5	BNU-ESM_SDSM_R85
CMCC-CESM	Centro Euro-Mediterraneo per I Cambiamenti Climatici	Italy	AEMET analog	8.5	CMCC-CESM_AN_R85
			SDSM	8.5	CMCC-CESM_SDSM_R85
MPI-ESM-LR	Max-Planck-Institut für Meteorologie	Germany	AEMET analog	4.5	MPI-ESM-LR_AN_R45
				8.5	MPI-ESM-LR_AN_R85
			SDSM	4.5	MPI-ESM-LR_SDSM_R45
				8.5	MPI-ESM-LR_SDSM_R85
MPI-ESM-MR	Max-Planck-Institut für Meteorologie	Germany	AEMET analog	4.5	MPI-ESM-MR_AN_R45
				8.5	MPI-ESM-MR_AN_R85
			SDSM	4.5	MPI-ESM-MR_SDSM_R45
				8.5	MPI-ESM-MR_SDSM_R85

Table 3. Most sensitive parameters (ranked from 1 the most sensitive and 13 the less sensitive) in the Upper Nerbioi River catchment, their description, the range used for the autocalibration (p-factor 0.81 and r-factor 0.41) and the best value.

Change type	Variable name	Description	Range	Best value
r	CN2	Curve number	-0.2-+0.2	-0.07
v	ESCO	Soil evaporation compensation factor	0.77-0.86	0.83
v	GWQMN	Depth of water in the shallow aquifer required for return flow to occur	614-655	625.36
r	SOL_AWC	Available water capacity	0.1-0.5	0.48
v	EPCO	Plant uptake compensation factor	0.8-0.95	0.87
v	REVAPMN	Threshold water in shallow aquifer	768-900	892.21
v	CH_K2	Main channel conductivity	10-44	38.66
v	ALPHA_BF	Base flow alpha factor	0.6-0.9	0.77
v	SURLAG	Surface runnoff lag coefficient	0.5-2.5	1.32
v	SMTMP	Snow melt base temperature (ºC)	3-9	4.77
v	GW_DELAY	Delay time for aquifer recharge	1-20	1.4
v	SFTMP	Snowfall temperature (ºC)	0.39-1.5	0.62
v	GW_REVAP	Groundwater “revap” coefficient	0.017-0.04	0.026

“v” means the default parameter is replaced by a given value; “r” means the existing parameter value is changed relatively

Table 4. Values obtained for the statistical indices used in the evaluation of the SWAT model performance at daily time-step. Seasonal statistical values are calculated for the 1996-2013 period.

				DISCHARGE		
	Scale	**NSE**	**r2**	**slope/int.**	**PBIAS**	**RSR**
CALIBRATION	1996-2006	0.63	0.68	0.85/0.35	-1.00	0.61
VALIDATION	2007-2013	0.75	0.77	0.91/0.24	0.17	0.50
HIGH AI	2010-2012	0.67	0.76	1.02/0.16	-10.51	0.58
LOW AI	2003-2005	0.74	0.76	1.01/0.16	-5.16	0.51
ALL 1996-2013	1996-2013	0.69	0.72	0.89/0.3	-0.51	0.56
	WINTER	0.66	0.68	0.81/0.62	6.26	0.58
	SPRING	0.74	0.76	0.87/0.1	17.74	0.51
	SUMMER	0.29	0.40	0.61/0.06	12.23	0.84
	AUTUMN	0.61	0.72	0.98/0.77	-26.78	0.63

* According to Moriasi et al., (2007) the discharge simulation is satisfactory at monthly time step when the NSE > 0.5, r^2 > 0.5, RSR ≤ 0.7, and PBIAS < 25%. The best value for slope is 1 and 0 for intercept (Arnold et al., 2012).

Table 5. Sign (+ or -) and probability of occurrence (P) of the annual and seasonal trends detected for the duration (days) of the period below Q20 and above Q80 between 1961 and 2000. Trends with a P higher than 0.66 are represented in bold; positive values are italicised.

		OBS_SIM	ACCESS1-0_AN	BNU-ESM_AN	BNU-ESM_SDSM	MPI-ESM-RL_AN	MPI-ESM-RL_SDSM	MPI-ESM-MR_AN	MPI-ESM-MR_SDSM	CMCC-CESM_AN	CMCC-CESM_SDSM
Q20	YEAR	0.39	0.58	0.34	***0.91***	-0.45	***0.73***	-0.45	0.50	***0.93***	*0.34*
	AUTUMN	-0.52	0.26	-0.08	0.37	-0.06	0.47	**-0.99**	0.04	*0.65*	***0.96***
	WINTER	*0.61*	0.00	0.00	0.00	0.00	0.00	0.00	0.00	*0.00*	*0.00*
	SPRING	***0.86***	0.08	***0.68***	0.16	0.47	***0.73***	-0.40	**-0.81**	*-0.64*	*-0.05*
	SUMMER	0.32	-0.21	0.52	***0.85***	**-0.78**	0.45	0.41	***0.81***	*-0.64*	*-0.41*
Q80	YEAR	**-0.99**	-0.17	**-0.91**	**-0.90**	0.02	0.02	0.32	0.47	0.37	0.34
	AUTUMN	**-0.75**	0.50	**-0.98**	**-1.00**	**-0.75**	-0.50	0.25	***0.71***	-0.62	-0.52
	WINTER	**-0.68**	**-0.76**	0.49	0.63	***0.76***	0.62	-0.28	-0.49	-0.62	0.53
	SPRING	**-0.74**	-0.64	0.00	-0.48	-0.42	0.37	0.65	0.37	***0.77***	0.39
	SUMMER	**-0.91**	0.00	**-0.84**	**-0.85**	0.00	0.09	0.00	0.00	-0.35	0.00

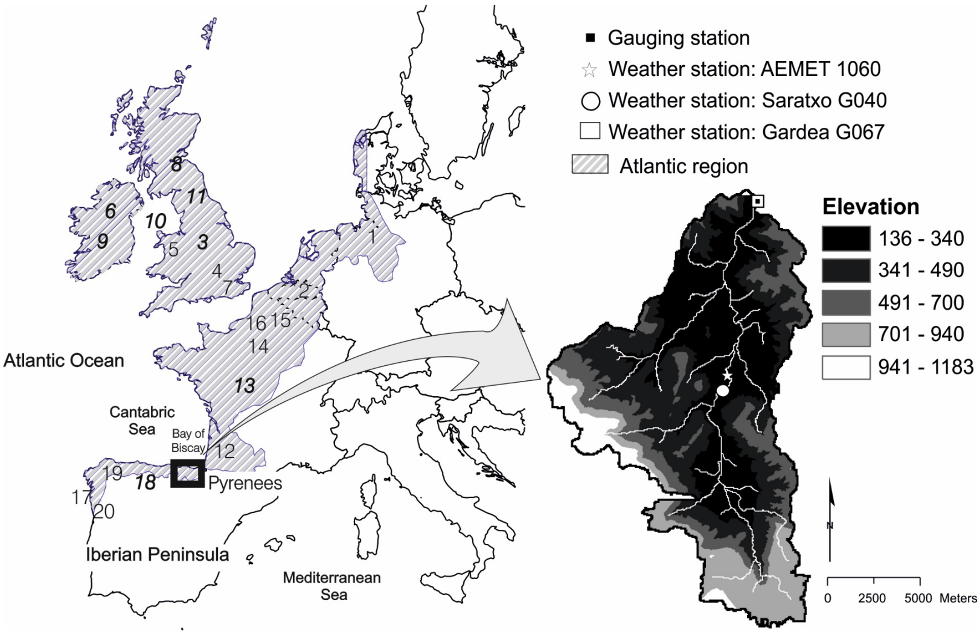

Fig. 1. Atlantic region area as described by the IPCC (2007). The location of the research works summarized in Table 1 is represented in by numbers. The italicised numbers in bold refer to works carried out in more than two catchments. Location of the Upper Nerbioi in this context and a map of river catchment with hydro-meteorological stations settings are also included.

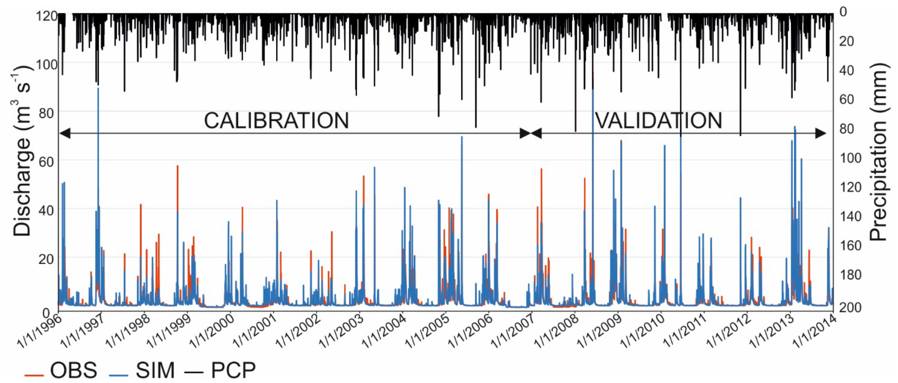

Fig. 2. Daily observed (OBS) and simulated (SIM) discharge for both the calibration (1996-2006) and the validation (2007-2013) periods, and the precipitation (PCP) observed in Amurrio station (AEMET 1060).

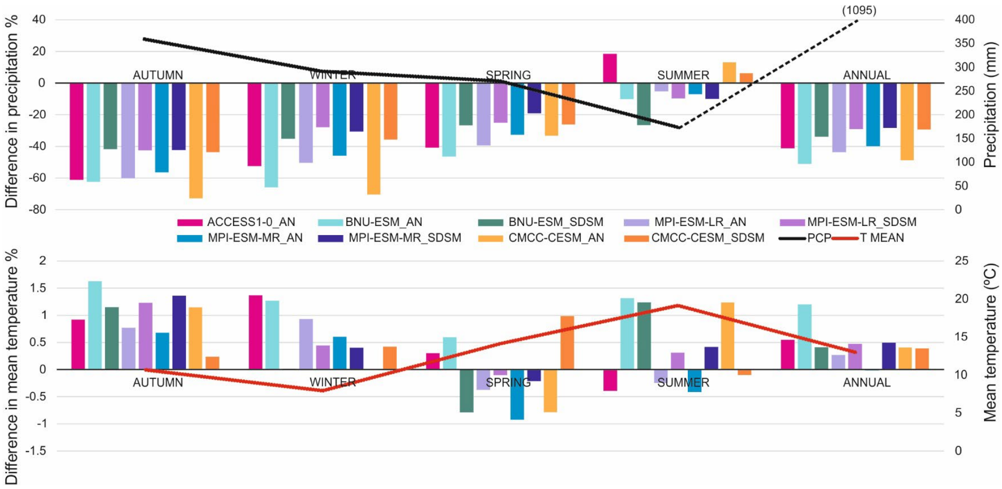

Fig. 3. Difference between observed meteorological parameters; precipitation (PCP) and average temperature (TMEAN) and climate baselines (1961-2000) before applying bias correction at annual and seasonal scales.

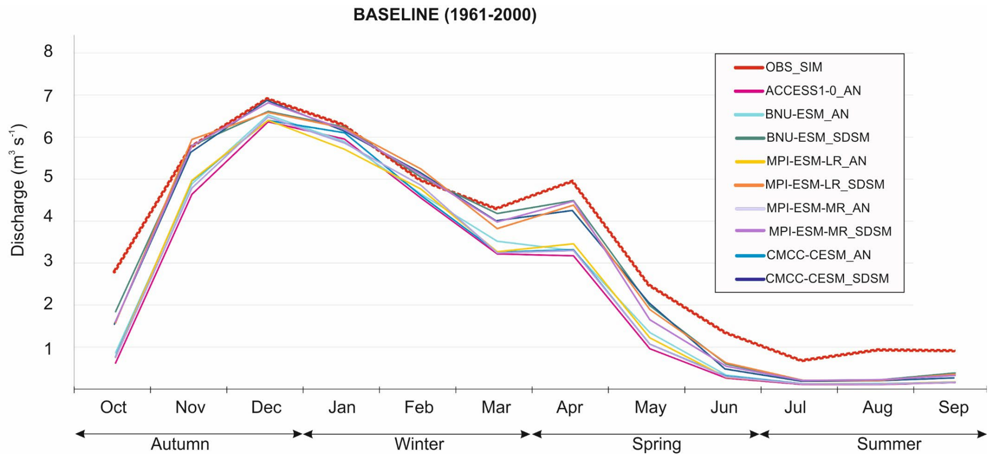

Fig. 4. Monthly mean discharge (m^3 s^{-1}) from 1961 to 2000 obtained from the hydrological simulation with observed meteorological data (OBS_SIM) and from the hydrological simulation with the downscaled GCMs baselines.

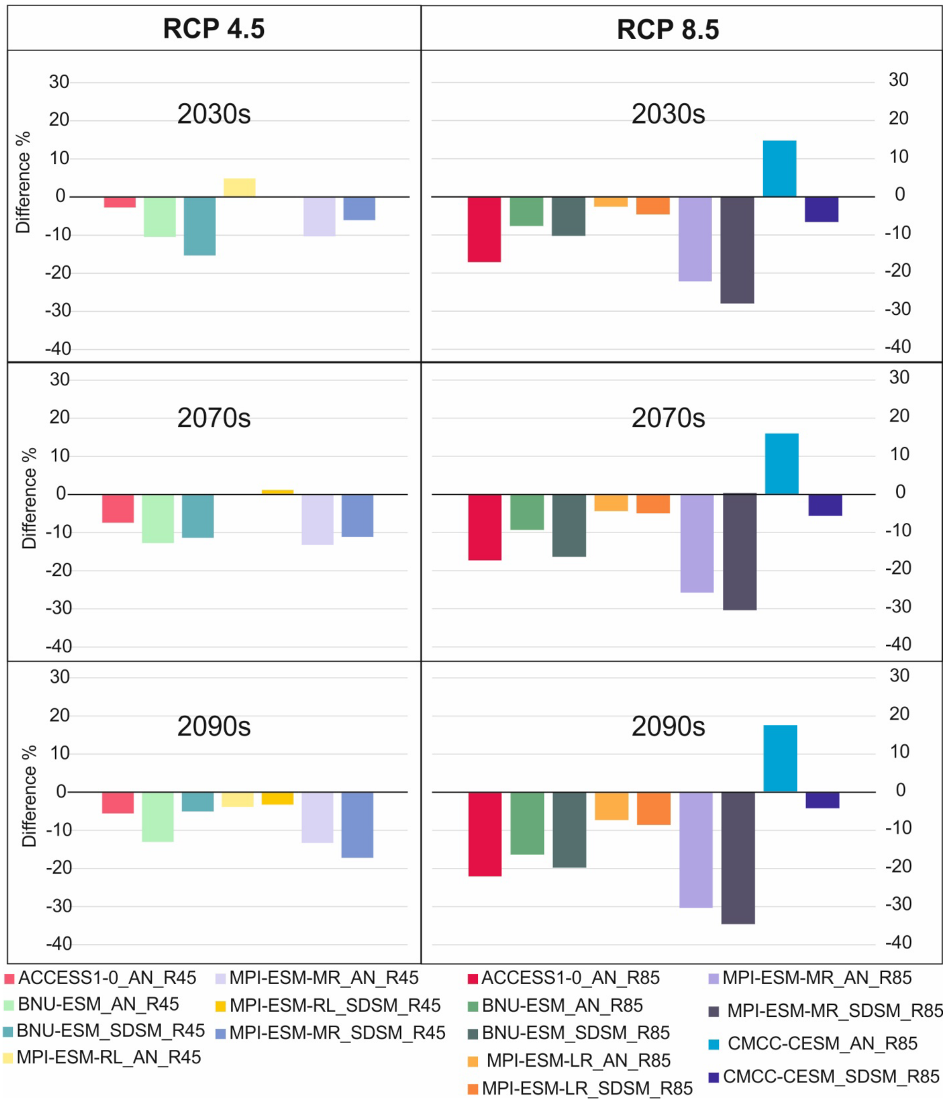

Fig. 5. Annual discharge difference (%) between the 16 hydrological projections and its respective baseline simulations, divided into three 30-year horizons (2030s, 2060s, 2090s).

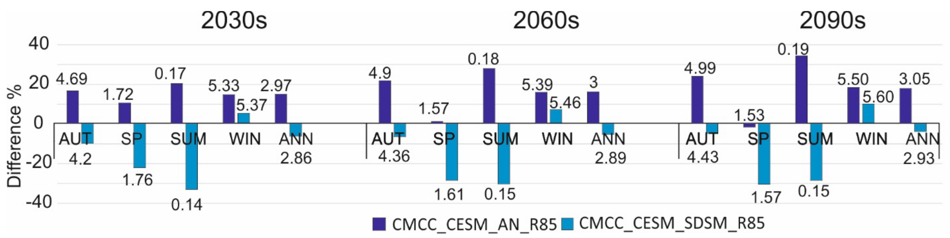

Fig. 6. Seasonal discharge difference (%) between CMCC_CESM_AN_R85 and CMCC_CESM_SDSM_R85 hydrological projections and their respective baselines divided into three 30-year horizons (2030s, 2060s, 2090s). In addition, the mean annual and seasonal discharge (m^3s^{-1}) is indicated in each bar.

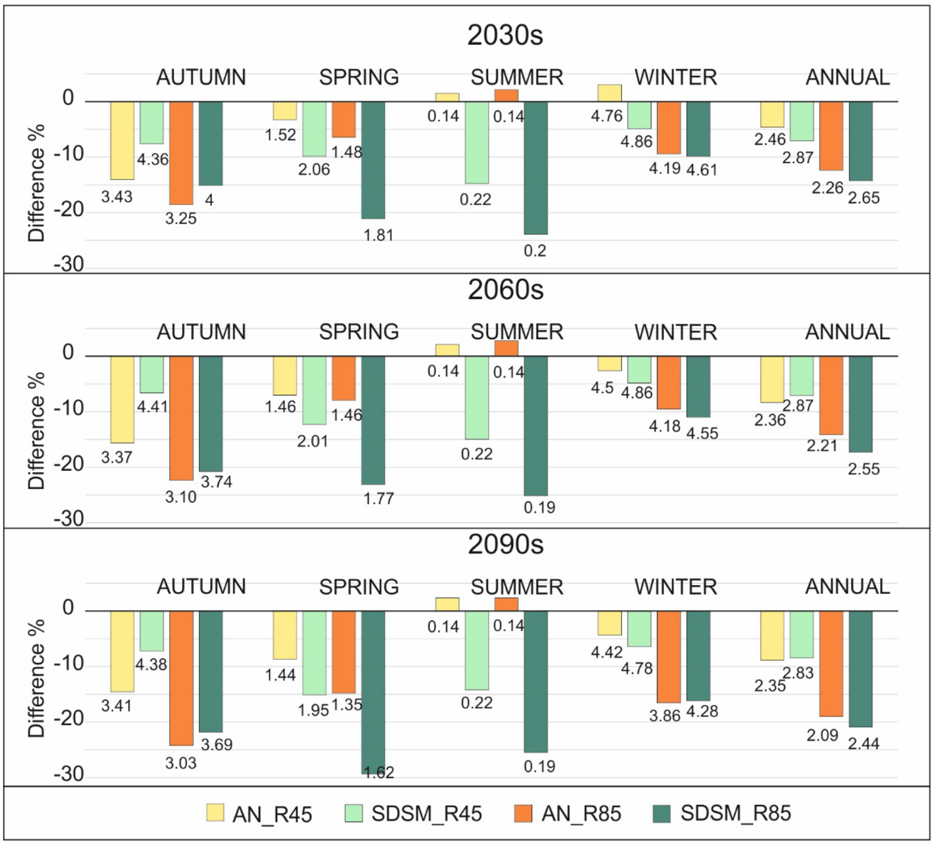

Fig. 7. Annual and seasonal discharge difference (%) between hydrological projections and their respective baselines grouped by downscaling method and RCP. The figure shows the mean difference between:

- ACCES1-0_AN_R45, BNU-ESM_AN_R45, MPI-ESM-MR_AN_R45 and MPI-ESM-RL_AN_R45, represented as **AN**_R45.
- BNU-ESM_SDSM_R45, MPI-ESM-MR_SDSM_R45 and MPI-ESM-RL_SDSM_R45, represented as **SDSM_R45.**
- ACCES1-0_AN_R85, BNU-ESM_AN_R85, MPI-ESM-MR_AN_R85 and MPI-ESM-RL_AN_R85, represented as **AN_R85.**
- BNU-ESM_SDSM_R85, MPI-ESM-MR_SDSM_R85 and MPI-ESM-RL_SDSM_R85, represented as **SDSM_R85.**

The results are divided into 3 horizons (2030s, 2060s, 2090s). In addition, the mean annual and seasonal discharge ($m^3 s^{-1}$) is indicated in each bar.

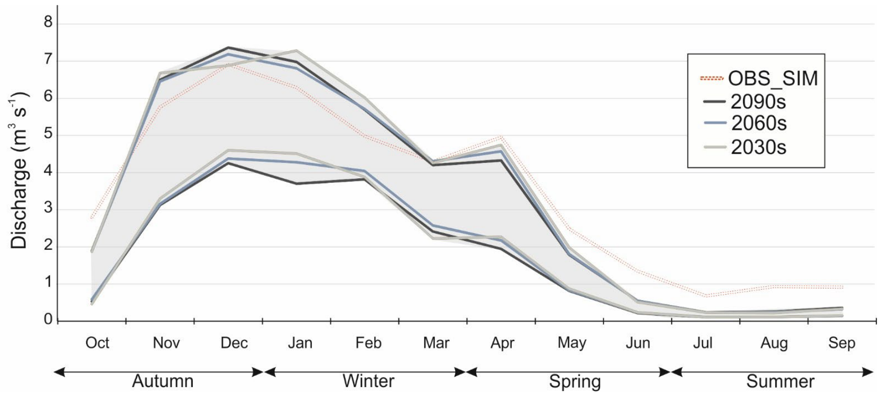

Fig. 8. Mean monthly discharge (m^3 s^{-1}) simulated with 16 climate projections. The highest discharge values represent the maximum value of the mean monthly discharge of all the projections by month, while the lowest values represent the minimum. The results are divided into three 30-year horizons (2030s, 2060s, 2090s). The grey colour represents the range of possible discharge values and the observed mean monthly discharge (1961-2000) is shown (OBS_SIM).

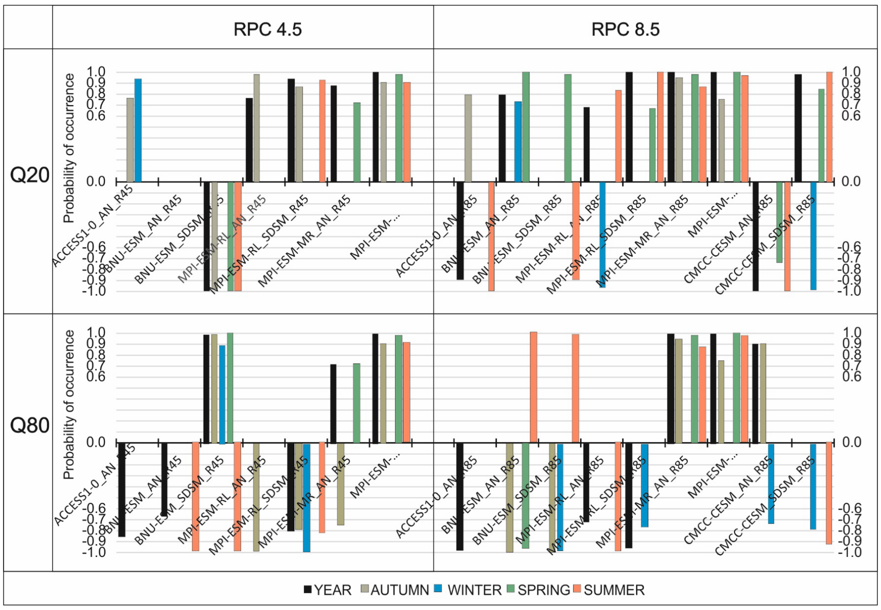

Fig. 9. Trends for low flow (Q20) duration and high flow (Q80) duration displayed at annual and seasonal scales for the 2011-2100 period. The projections under Representative Concentration Pathway 4.5 (RCP 4.5) and 8.5 (RCP 8.5) are displayed separately. Only values with a probability of occurrence higher than 0.66 are shown.